Wavefront Aberrations

Ilaria Nardecchia
INFN-Roma Tor Vergata
ilaria.nardecchia@roma2.infn.it

Ettore Majorana Centre for Scientific Culture

STGWD - Erice, 20-27 May 2026

Outline

- Gravitational Wave Detector Core Optics
  - Cold defects: Real Mirrors vs Ideal Design
- Thermal effects
  - simulations
- Impact of thermal effects on the ITF operation
  - Interferometer simulation tool
- Thermal compensation system (TCS)
  - Advanced Virgo case
- Next-generation wavefront actuators
- acronyms & references

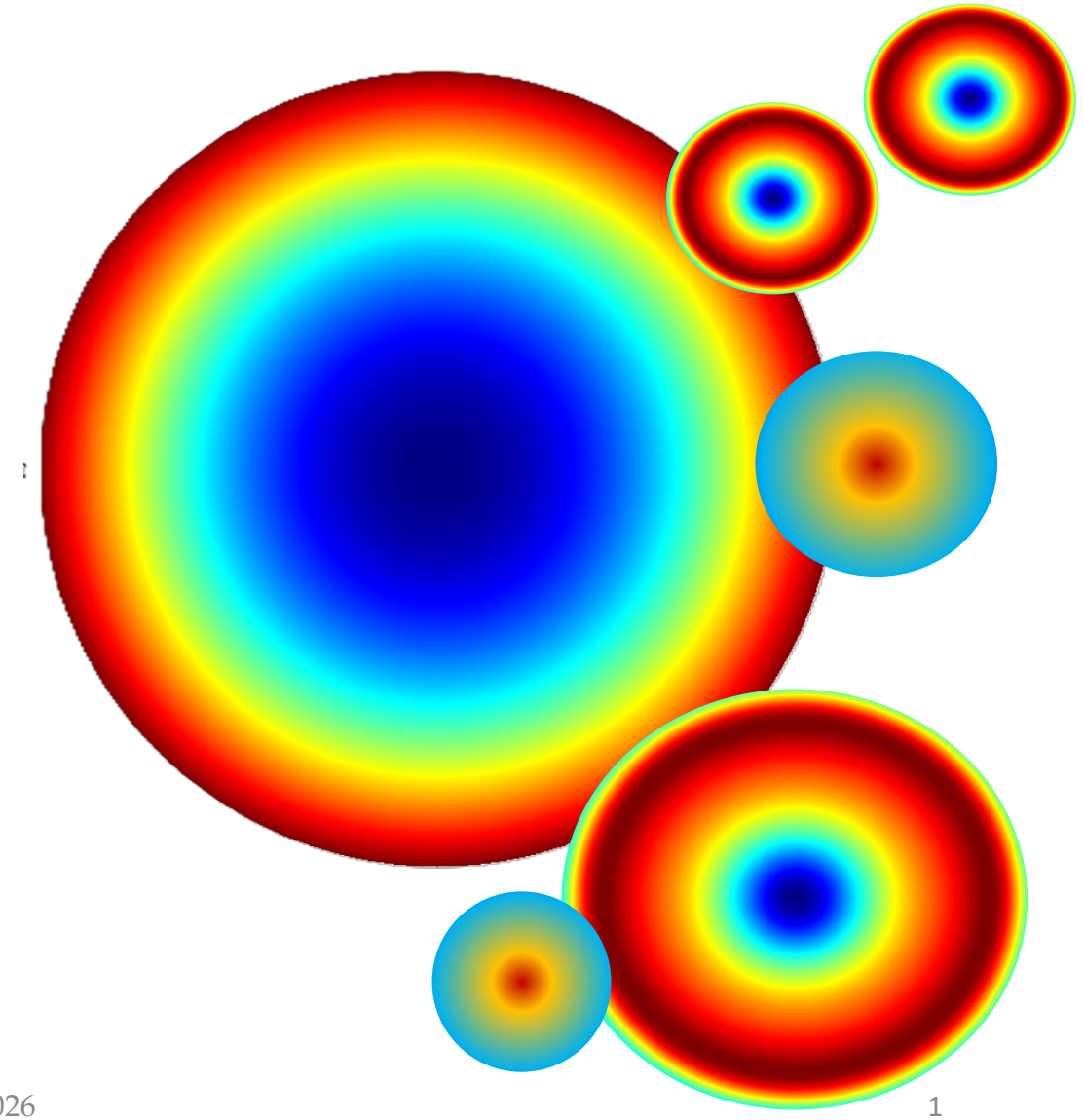

GW Detector Core Optics

- **Substrate**
  - High-purity fused silica (Suprasil)
  - Diameter: 35 cm, Mass: ~ 40 kg
- **Geometry**
  - Radius of Curvature (RoC): ~ 1.5 km
- **Manufacturing**
  - Substrates provided by Heraeus (Germany)
  - Polished by ZYGO (USA)
  - Coated by LMA (Lyon, France)
- **Coating**
  - High- and low-index amorphous oxide multilayers
  - High-Reflective (HR) / Anti-Reflective (AR) surfaces
  - Optical absorption: ~ 0.5 ppm

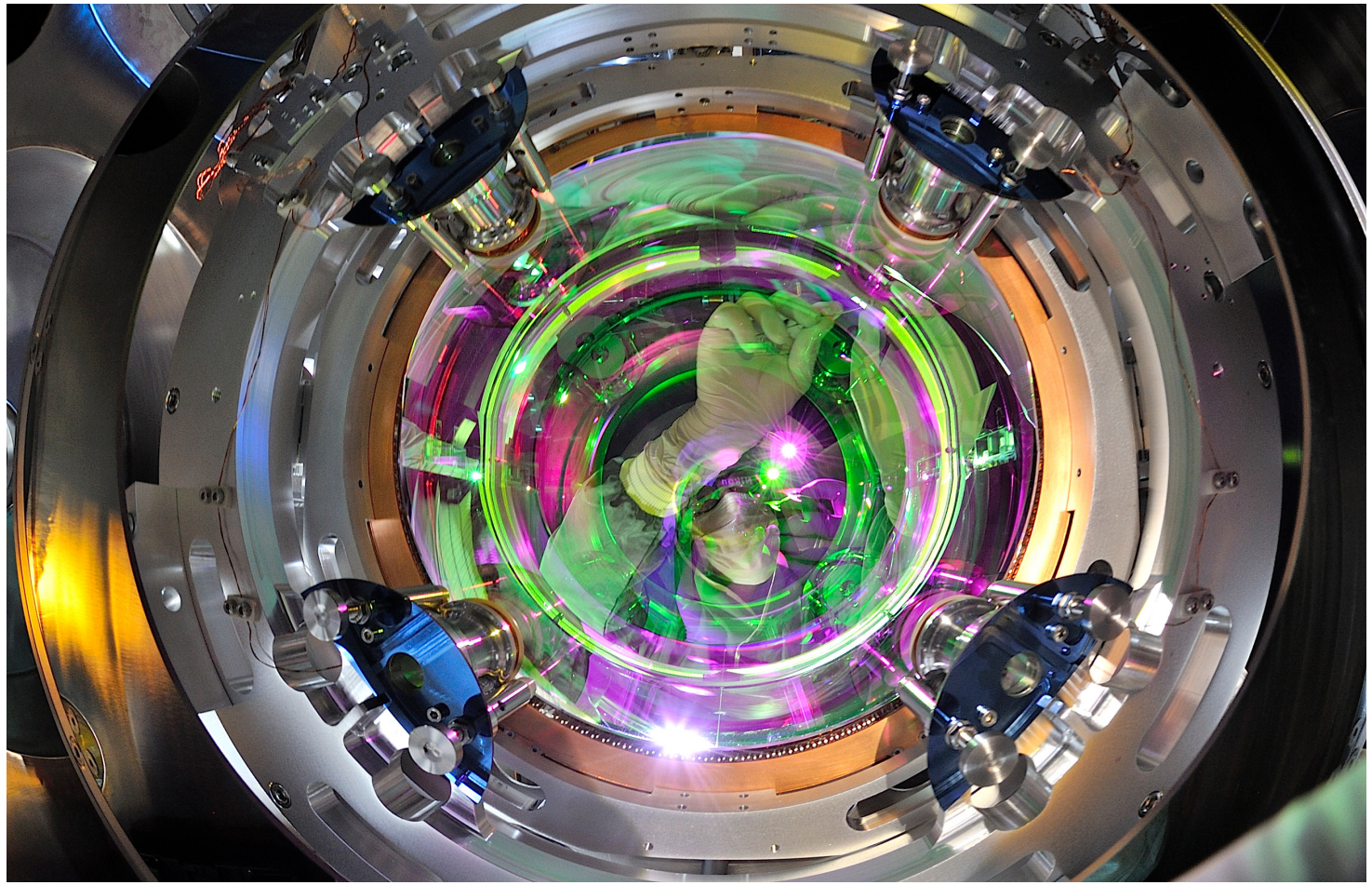

Credit by Maurizio Perciballi

Cold Defects: Real Mirrors vs Ideal Design

- Real mirrors deviate from the ideal design due to residual manufacturing imperfections:
  - Substrate inhomogeneities
  - Surface figure errors
- Consequences:
  - Optical Path Length (OPL) distortions on the main YAG beam
  - Deviations from the nominal RoC

Example of substrate inhomogeneities map in Advanced Virgo core optics

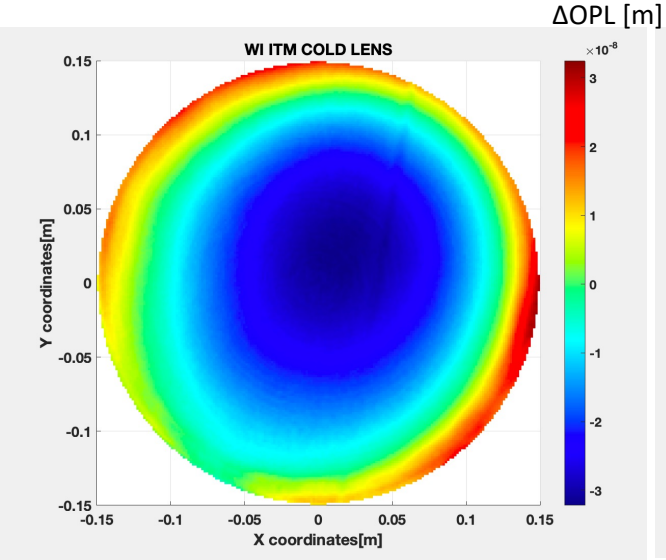

Example of surface figure errors map in Advanced Virgo core optics

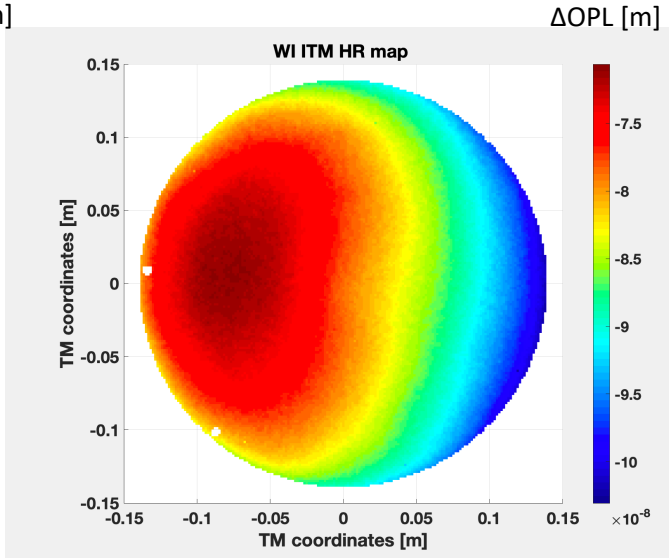

Mirror quality is critical: manufacturing imperfections directly affect interferometer performance

Thermal effects

- When the ITF reaches its final working point → high circulating power → the mirror coating heats up and the absorbed heat diffuses into the substrate

- Thermal lensing

$$\Delta OPL_{TL} = (2\,\frac{dn}{dT} + (n-1)(1+\sigma)\,\alpha)\int_0^h \Delta T\, dz$$

Dominant contribution

  - **dn/dT=**9.8 x 10^{-6} 1/K,
  - Refractive index: n=1.452
  - Poisson ratio: σ=0.17
  - Thermal expansion coefficient: α=0.55 x 10^{-6} 1/K

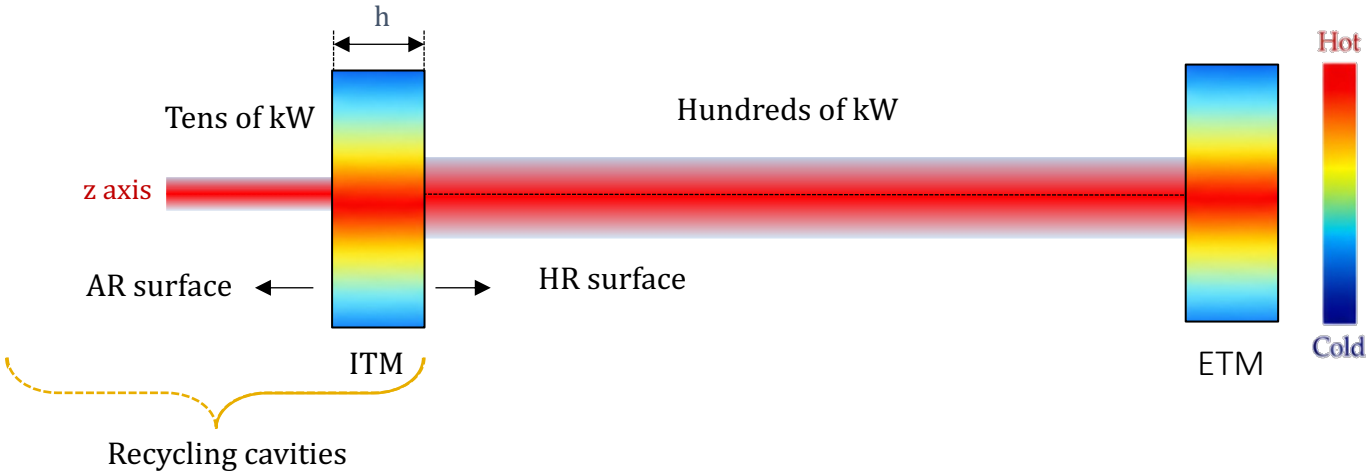

- Thermo-elastic deformation of the ITM and ETM HR surfaces (α ≠0)

$$\Delta OPL_{TE} = 2\,\alpha \int_0^h \Delta T\, dz$$

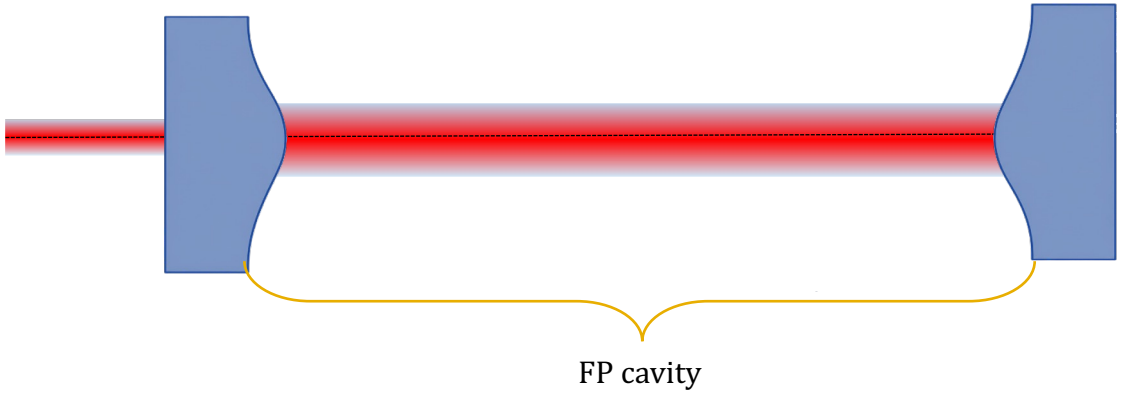

Thermal Lensing Simulations

EXAMPLE WORKING POINT:
- Injected power ~18 W
- Absorbed power ~60 mW

Simulation workflow:

Temperature map [Finite Element Analysis (FEA)] → Optical Path Length variation ΔOPL → Gaussian-weighted quadratic fit → Equivalent thermal lens

Gaussian-weighted quadratic fit:

- The interferometer is most sensitive to the central region of the mirror

$$w(r) = \frac{1}{\pi\omega^2}\, e^{-2\frac{r^2}{\omega^2}}$$

(Gaussian weights defined by the beam intensity profile, w = beam radius)

Thermal lenses approximation:

- Thermal lenses can be treated as optical dioptres

$$Dp = \frac{1}{f} = 2\,a$$

f = focal length
a = quadratic coefficient of the parabolic fit

1) Example of FEA temperature distribution inside the ITM substrate

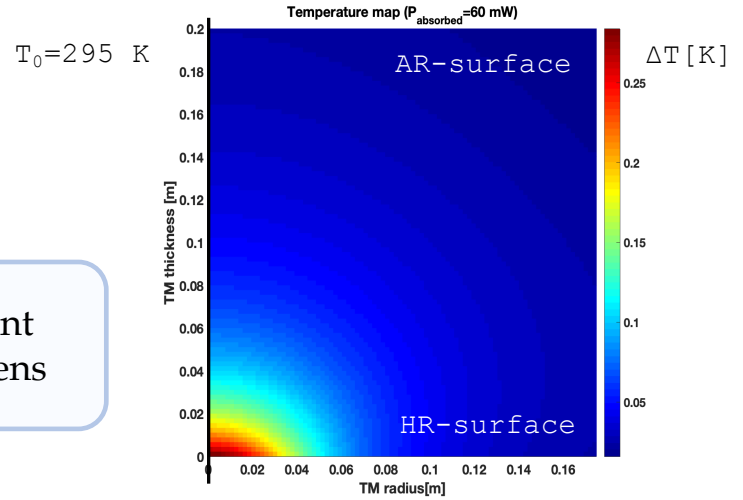

2) OPL radial profile and Gaussian-weighted quadratic approximation

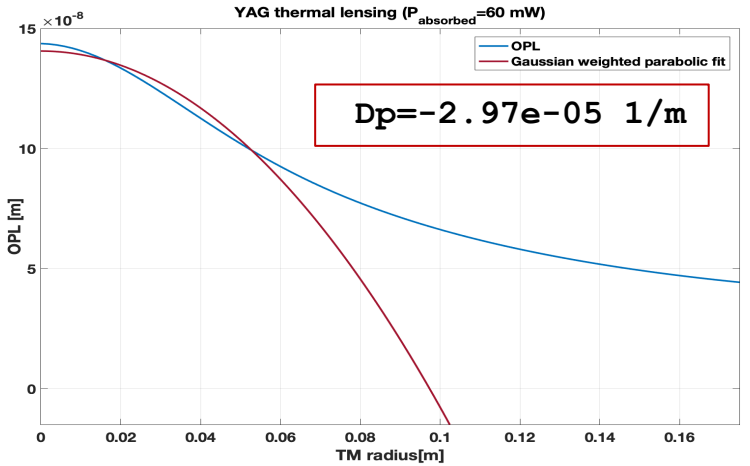

Thermo-elastic Simulations

- EXAMPLE WORKING POINT:
  - Injected power ~18 W
  - Absorbed power ~60 mW

Simulation workflow:

Temperature map [Finite Element Analysis (FEA)] → HR surface deformation [FEA] → Gaussian-weighted quadratic fit → ΔRoC

1) Example of FEA thermo-elastic deformation on the HR-surface

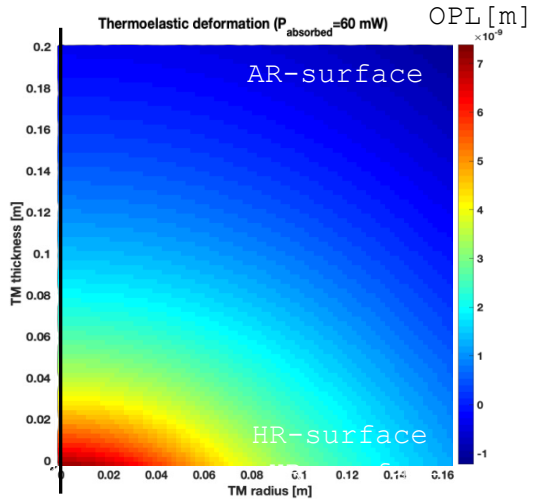

3) Gaussian-weighted quadratic fit:

- The interferometer is most sensitive to the central region of the mirror

$$w(r) = \frac{1}{\pi\omega^2}\, e^{-2\frac{r^2}{\omega^2}}$$

(Gaussian weights defined by the beam intensity profile, w = beam radius)

2) OPL radial profile and Gaussian-weighted quadratic approximation

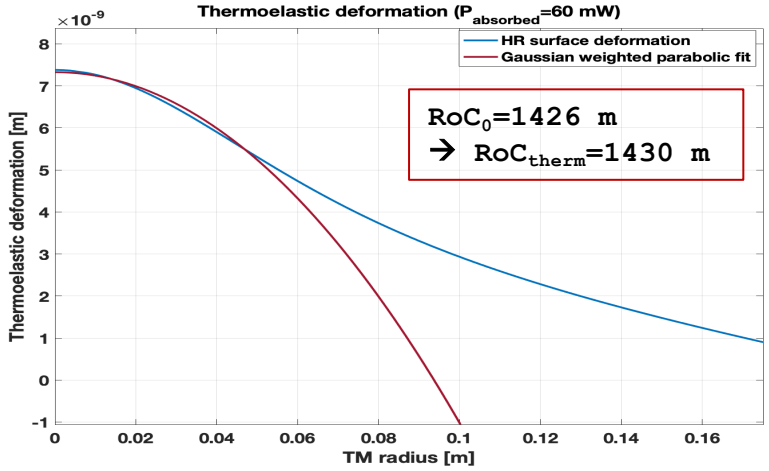

4) Spherical surface approximation:

- Thermo-elastic deformation

$$RoC = \frac{1}{2\,a}$$

a = quadratic coefficient of the parabolic fit

Thermal Lensing

- Thermal lensing in the input mirrors: dominant spherical component + **residual non-spherical component**

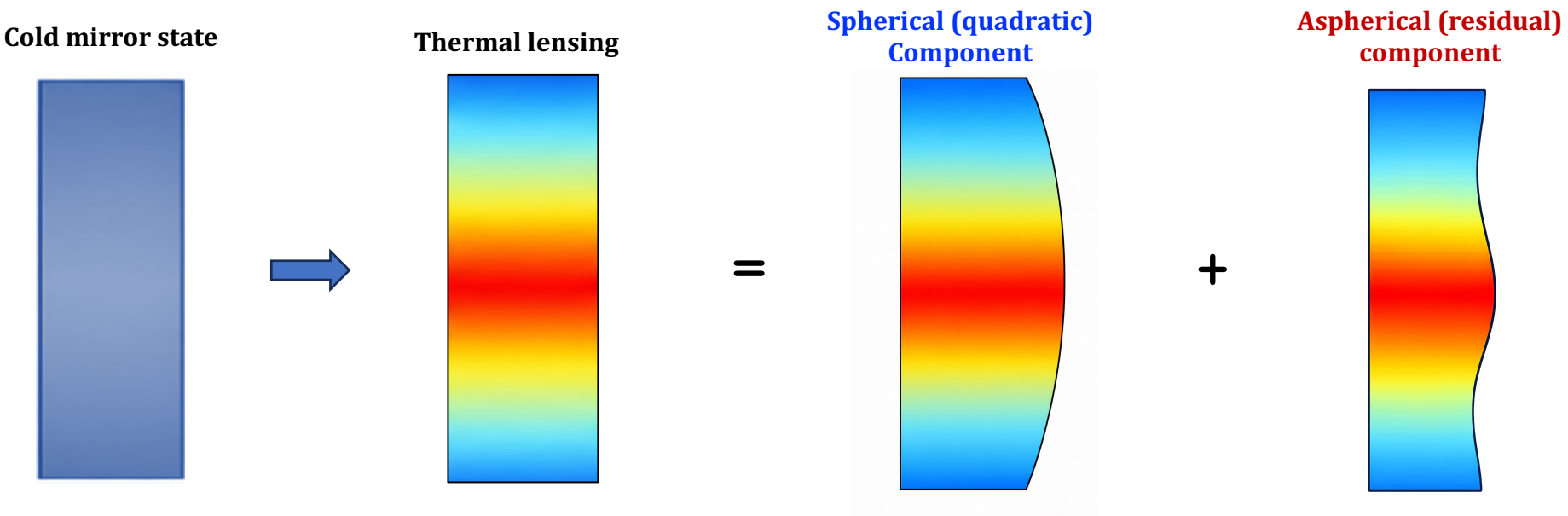

- Thermal lensing affects the recycling cavities and generates mode mismatch with the FP arm cavities

- The quadratic (spherical) fit captures only the dominant focusing term

Thermo-Elastic Effect on the HR-surface

- Thermo-elastic deformation on the HR-surface in the FP mirrors: dominant spherical component + **residual non-spherical component**

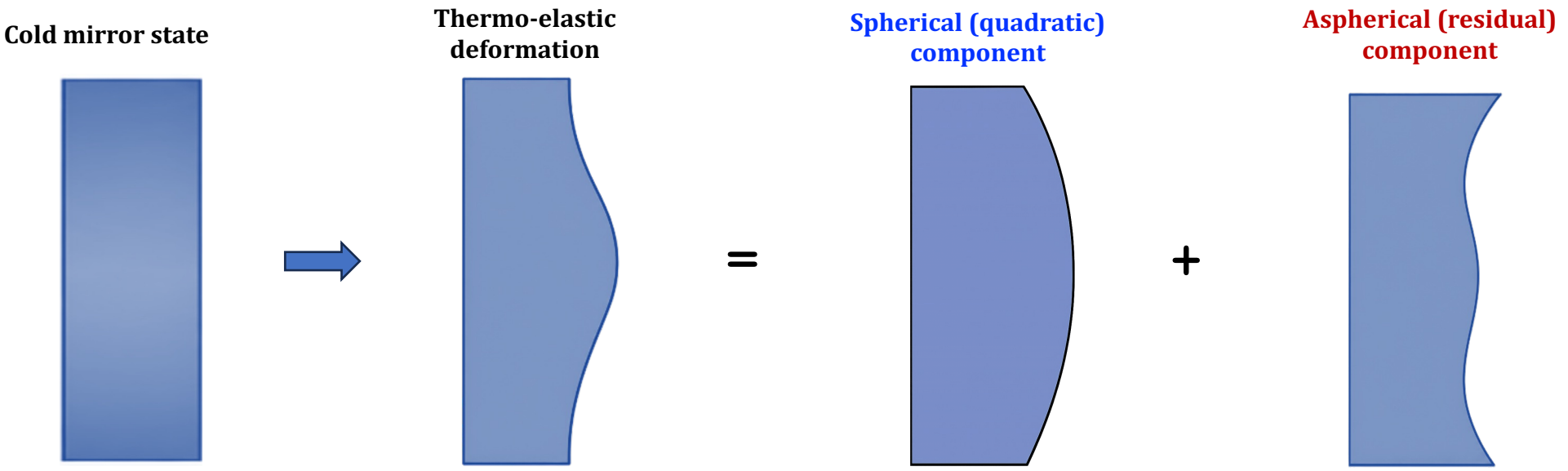

- Thermo-elastic deformation introduces wavefront distortions in the Fabry–Perot cavities

- The quadratic (spherical) fit captures only the dominant focusing term

Impact of thermal effects on the ITF operation

- Thermal lensing in the ITMs causes:
  - Mode mismatch with the FP cavities
  - HOMs resonating in the recycling cavities
  - Sideband power losses and their degradation for longitudinal/angular control

→ **Reduced ITF duty cyle**

- Thermo-elastic deformation of the HR-surfaces in all FP mirrors:
  - HOMs resonating in the FP cavities
  - Decrease of power circulating in the FP-cavities
  - Increase of shot noise

→ **Sensitivity degradation at high frequency**

- Cavity stability parameter (g) determines the filtering capability of HOMs

Input beam: TEM00+TEM01

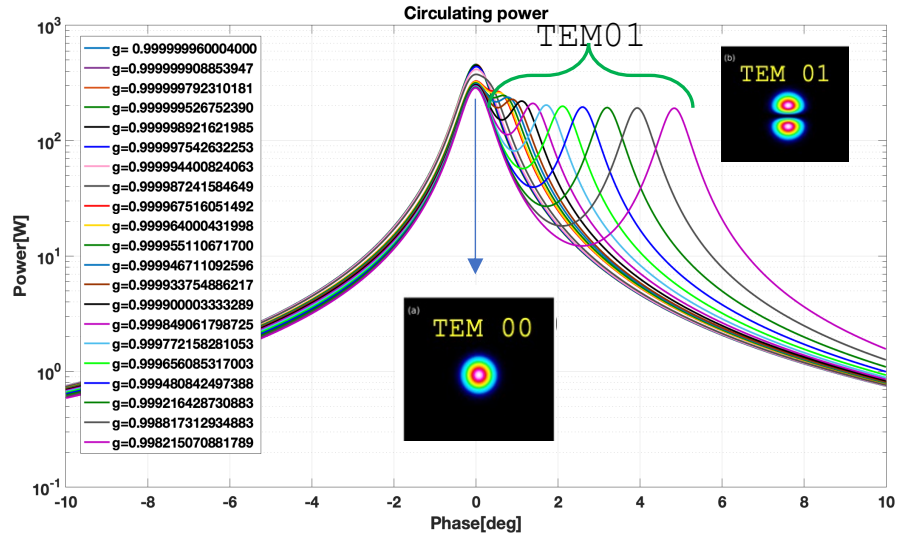

Power circulating in a generic cavity moving from the region close to the instability (g~1) toward the stable one.

Advanced Virgo case

- Optical configuration:
  - Fabry-Perot arm cavities are stable (g~0.8707)
  - PRC and SRC are marginally stable (g~0.9999885, very close to 1)
  - PRC and SRC are extremely sensitive to deviations from the nominal optical configuration:
    - Cold defects
    - Thermal effects
  - Even small HOM excitations can resonate inside the recyling cavities
  - After reaching the final working point, thermal effects arising in the input mirrors degrade the RF sidebands circulating in the recycling cavities

→ Loss of the interferometer working point after ~20-30 minutes

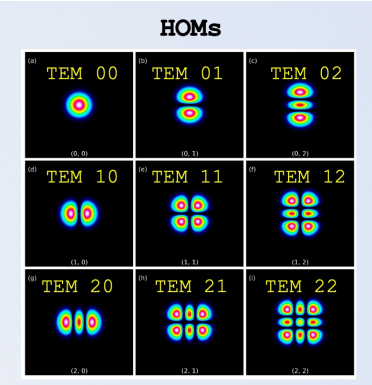

Sideband power evolution at the interferometer bright port after reaching the final working point

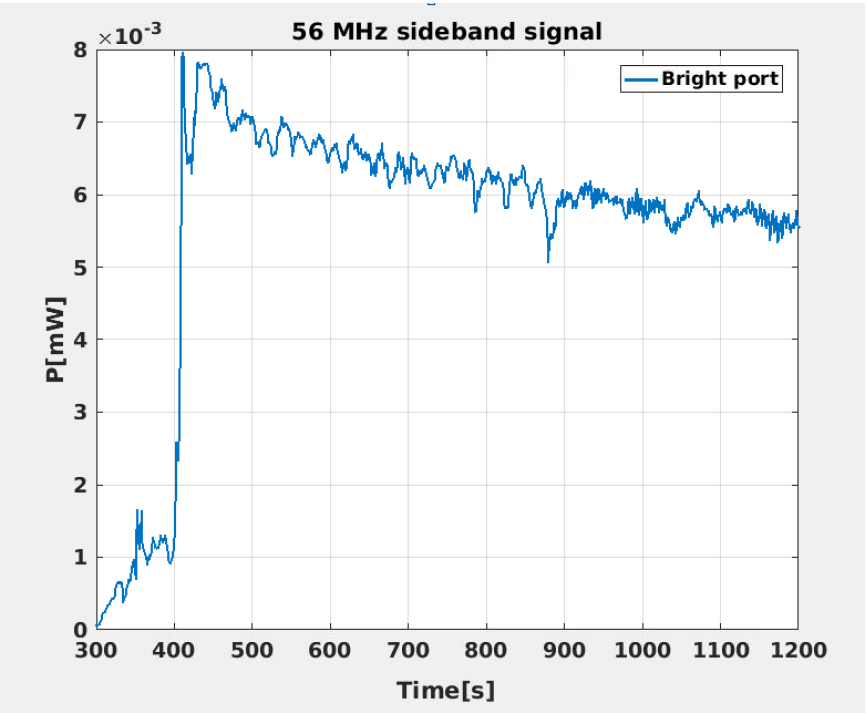

Interferometer simulation tool

- Full interferometer optical simulations are essential to identify the requirements for the wavefront aberration compensation

OSCAR

- Developed by **Jérôme Degallaix** within the Virgo Collaboration
- The code is publicly available on MATLAB File Exchange. (https://www.mathworks.com/matlabcentral/fileexchange/20607-oscar)

OSCAR is a
FFT optical simulation tool for gravitational-wave interferometers

MAIN CAPABILITIES

- Free-space propagation of laser beams
- Simulation of optical cavities with multiple mirrors
- Analysis of mirror surface maps
- Calculation of interferometer error signals

STEADY STATE SIMULATION OUTPUTS

- Optical power distribution (carrier and sidebands)
- 2D field and mode amplitudes
- Higher-order mode content

→OSCAR is extensively used for thermal compensation studies in Advanced Virgo

EXAMPLE OUTPUTS

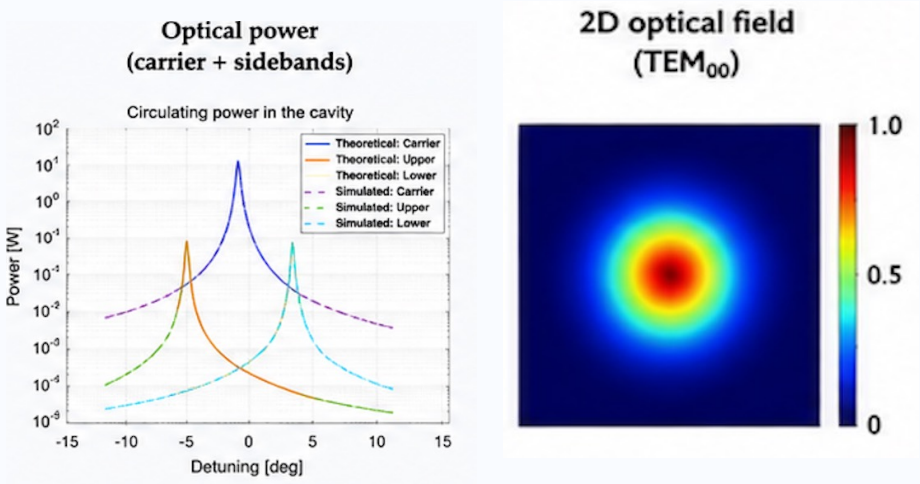

Thermal compensation system (TCS)

- **The Thermal Compensation System (TCS) compensates both cold defects and thermally induced deformations**
- The TCS generates an aberration equal and opposite to the thermal effect
- Mirrors are suspended so they cannot be touched
- The only non-contact way to heat the mirrors is via radiation
- Requirements on thermal lensing and RoC variations are set by the interferometer optical design.
  - For example in Advanced Virgo:
    - Thermal lensing residual < 2 nm RMS
    - Radius of curvature controlled within ± 2 m

Aberration compensation principle

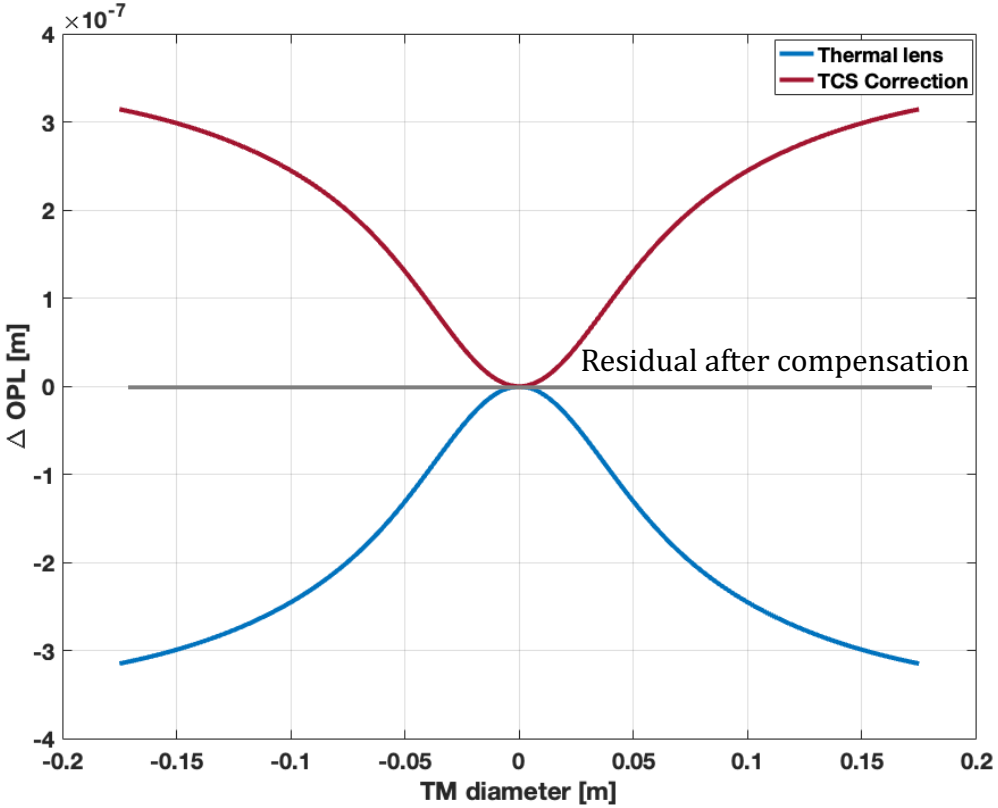

The TCS introduces an opposite aberration, leaving a minimum residual

Thermal Lensing compensation strategy

- **Thermal lensing in the mirrors**

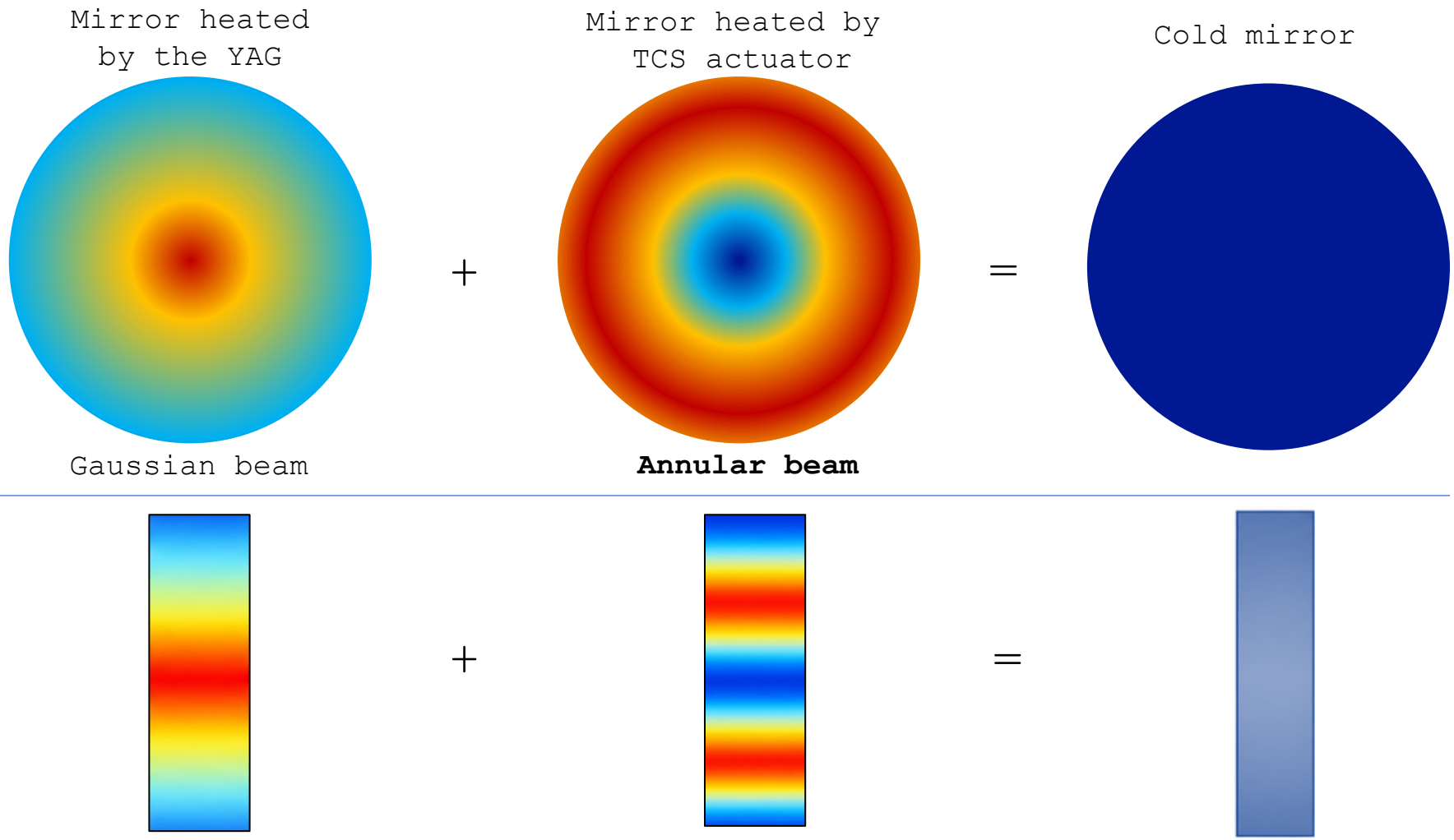

CO_2 Laser Projectors

- High-power CO_2 laser projectors are used to correct thermal lensing
- CO_2 wavelength (λ=10.6 μm) completely absorbed by fused silica
- Heating pattern projected onto the Compensation Plates (CPs) in order to avoid injecting noise into the FP cavities
- The heating profile is shaped to compensate for the distorsion
- An annular beam can be generated using an axicon (conical lens)
- Optimal heating pattern is achieved using a two-ring heating profile [Double Axicon System (DAS)]:
  - INNER RING → thick and weak
  - OUTER RING → thin and bright

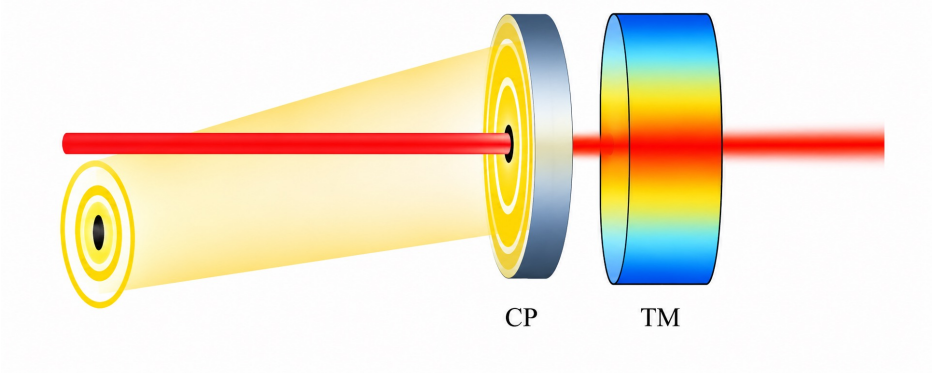

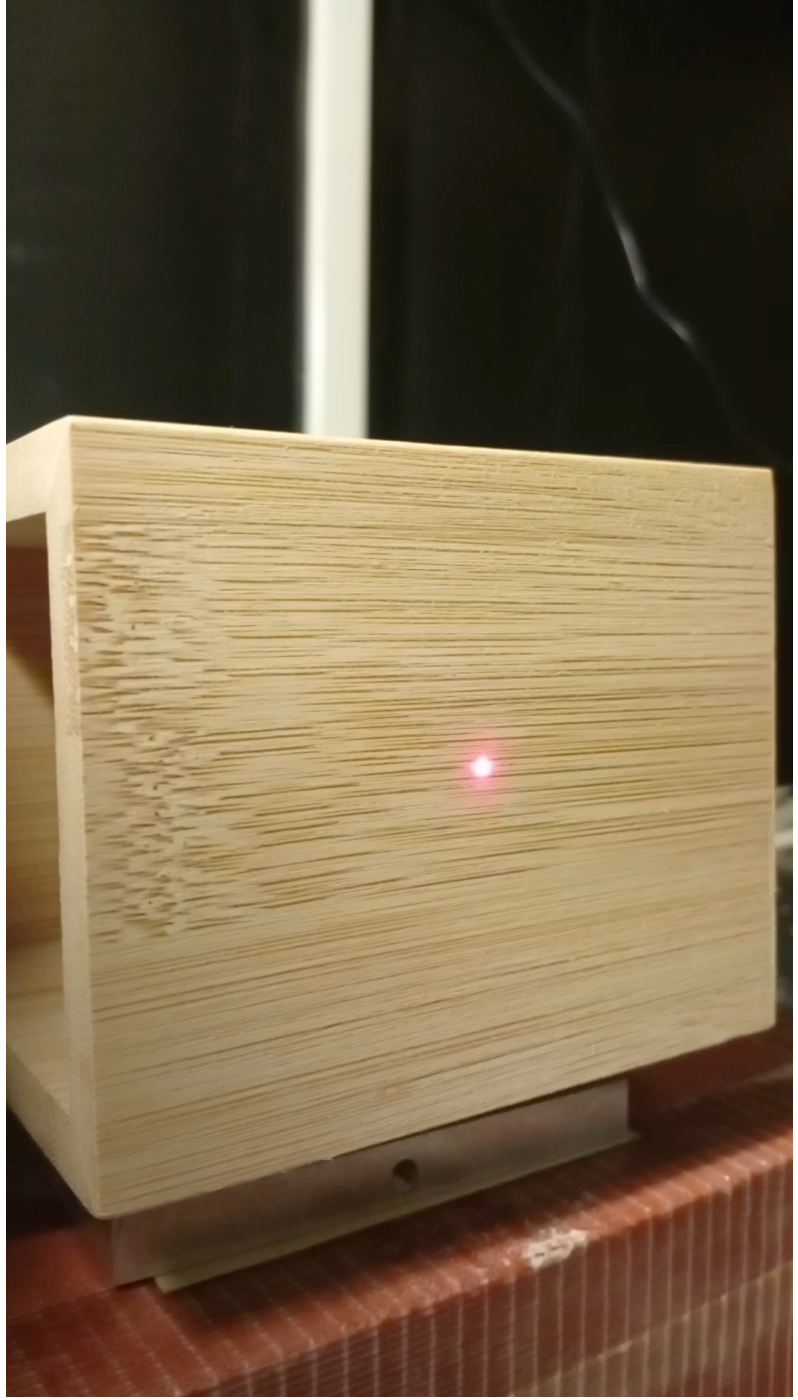

Credit by Luciano Antonio Corubolo

https://www.youtube.com/watch?v=BUUVRYy0y20

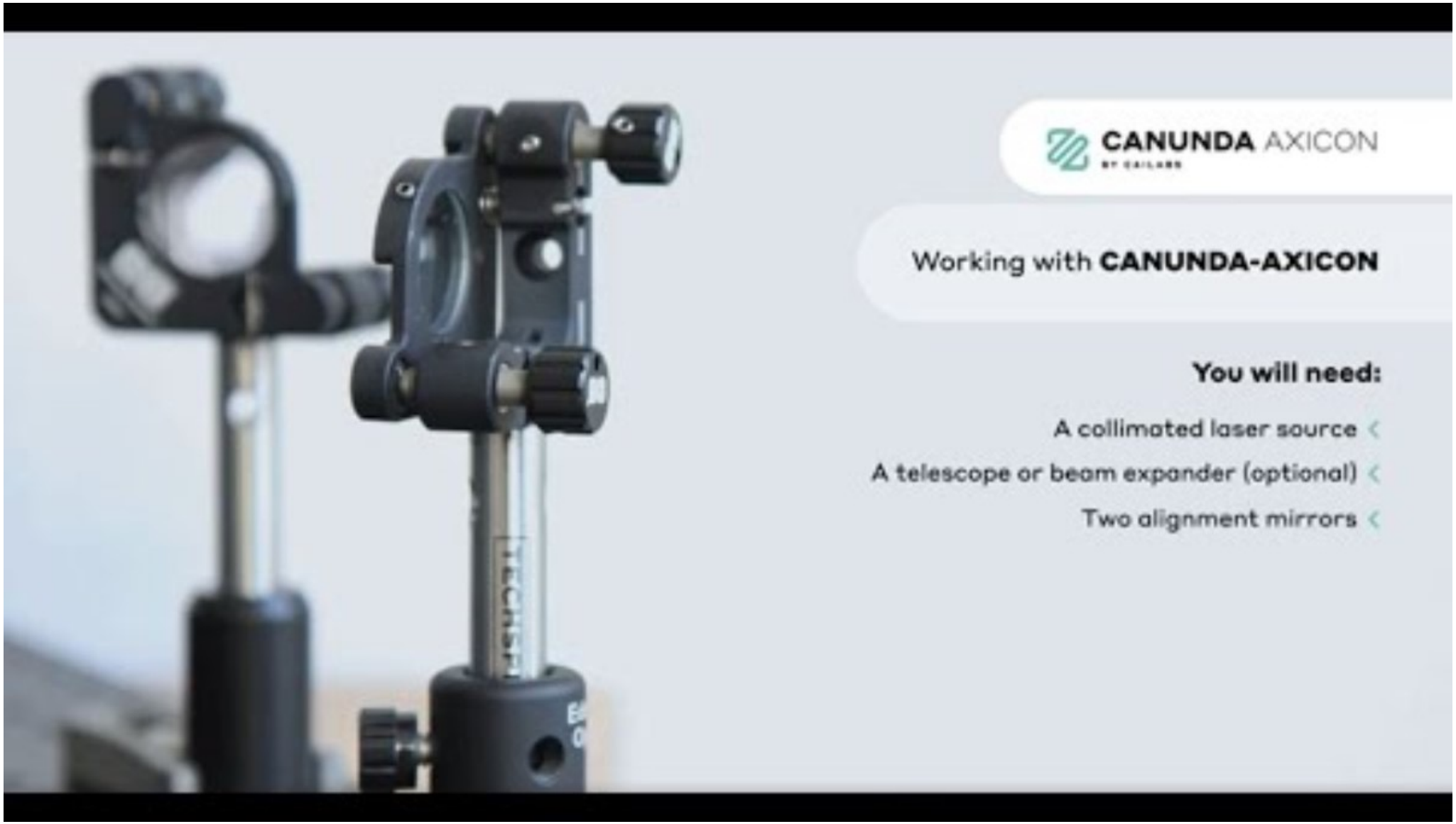

CO_2 Laser Projectors: Actuation Scheme

- The actuation scheme is designed to generate two independent heating patterns

Double Axicon System (DAS)

- Compensates thermal lensing due to uniform coating absorption

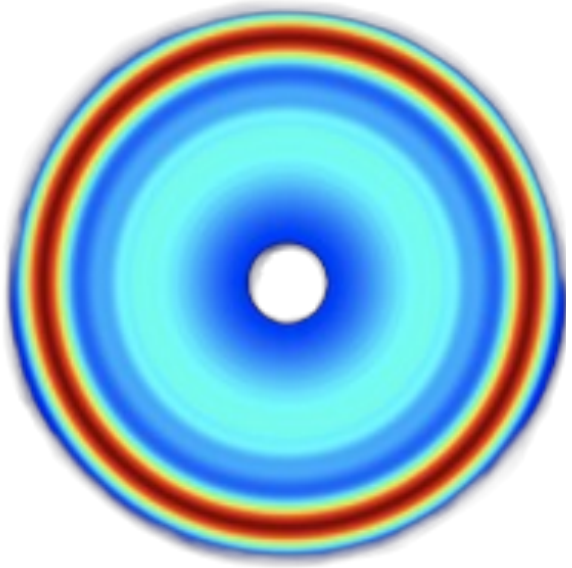

Central Heating (CH)

- Mimics the YAG thermal lens
- Used to mitigate thermal transients during loss of lock

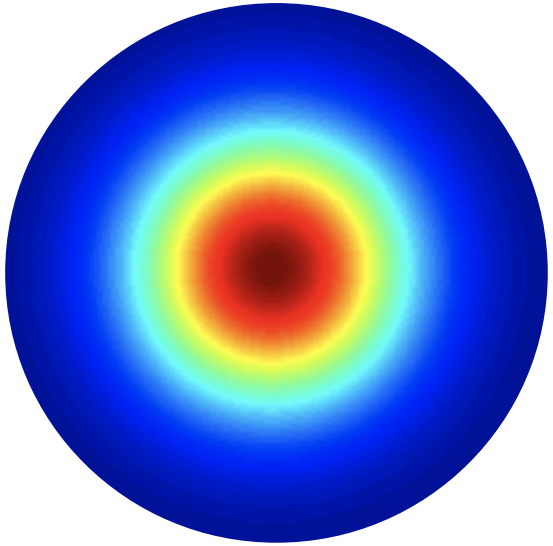

CO_2 Laser Projectors in Advanced Virgo

- Experimental implementation in Advanced Virgo

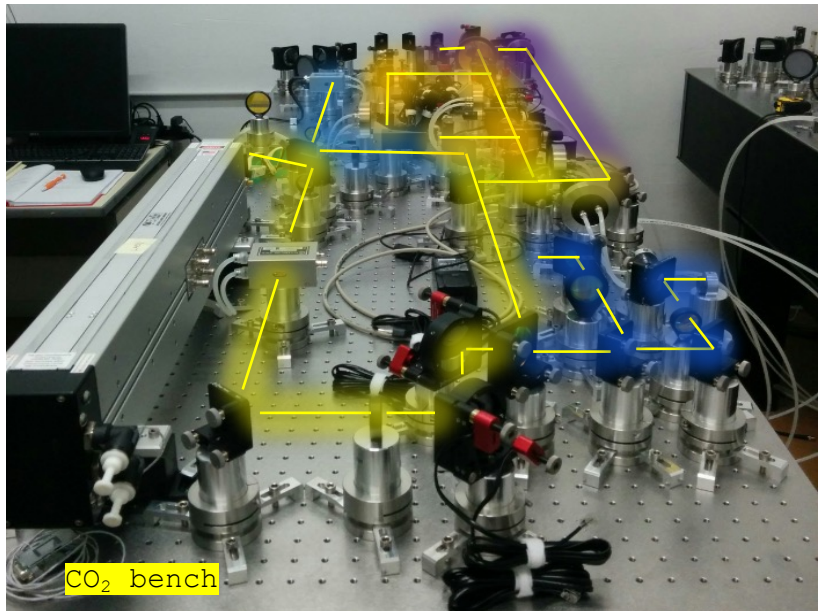
CO_2 bench

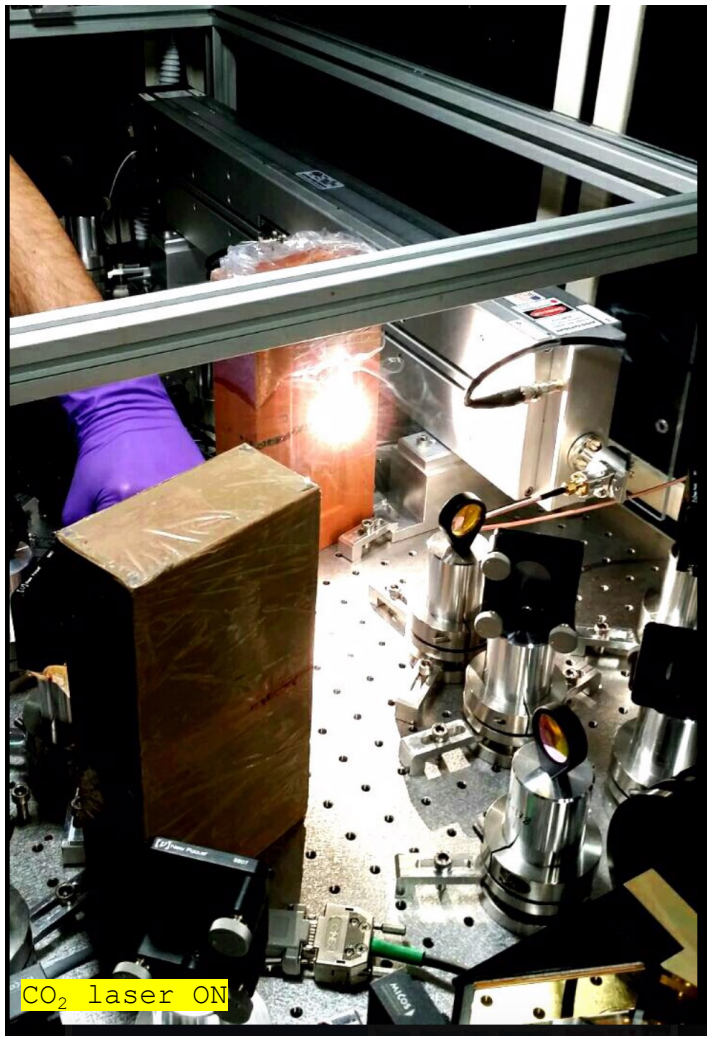
CO_2 laser ON

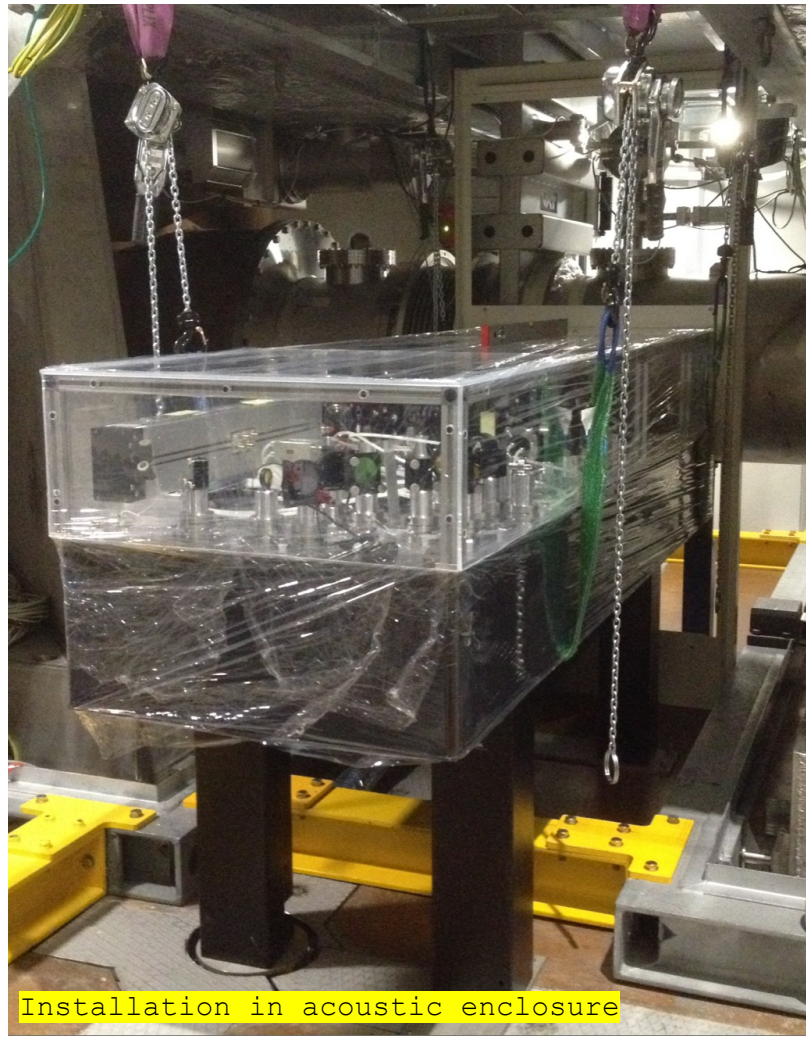
Installation in acoustic enclosure

Thermo-Elastic Effect on the HR-surface

- Thermo-elastic deformation on the HR-surface in the FP mirrors: dominant spherical component + **residual non-spherical component**

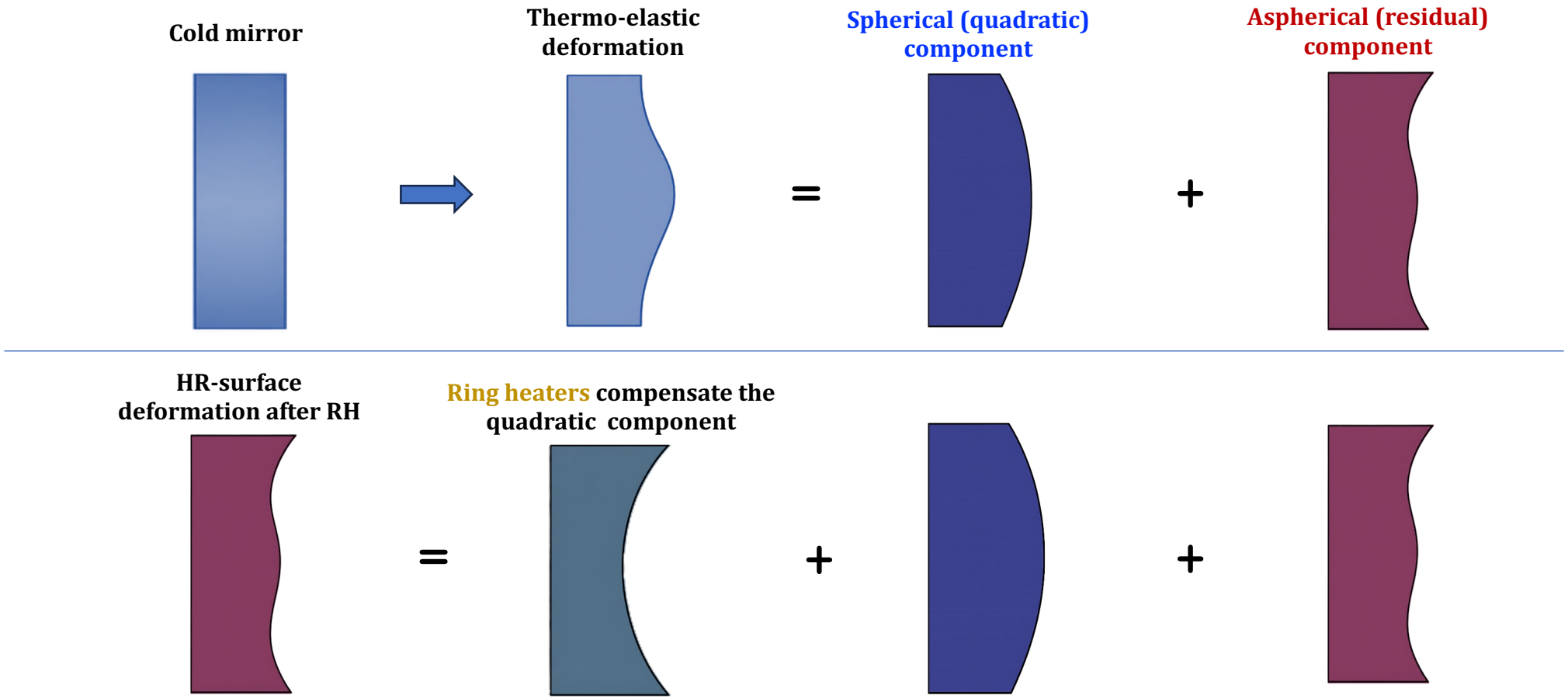

Thermo-Elastic Effect on the HR-surface

- Thermo-elastic deformation on the HR-surface in the FP mirrors: dominant spherical component + **residual non-spherical component**

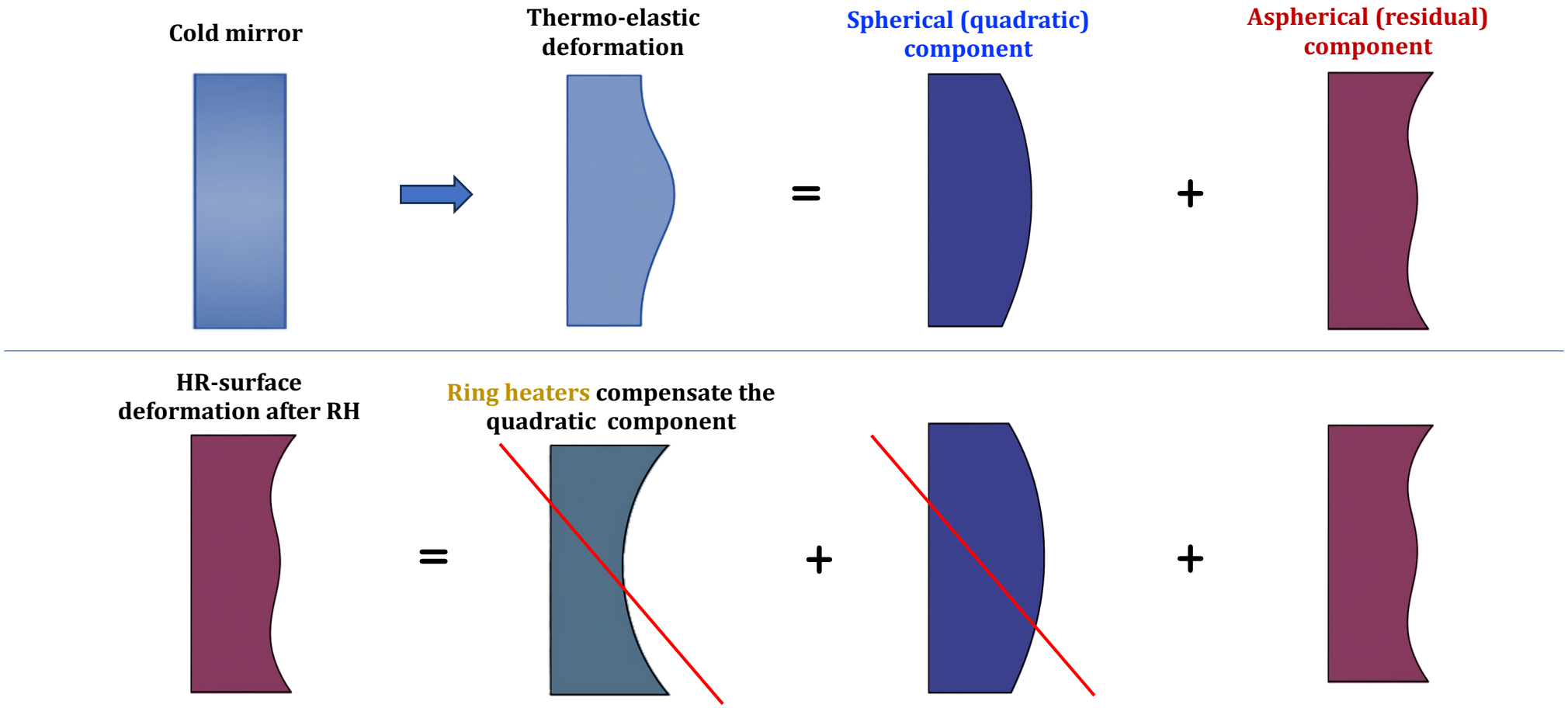

Ring Heater RADIATIVE PROJECTOR

- **Radiative actuator used to compensate thermo-elastic RoC variations.**
- The RH is a resistive heater installed around each mirror to heat the periphery of the optics.
- Main components:
  - 2 Pyrex Glass rings
  - NiCr conductive wire
  - Copper shield

Top view

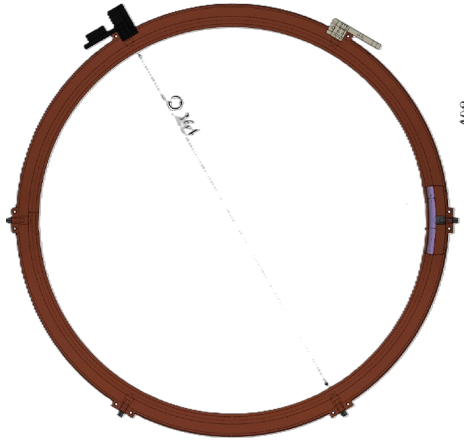

3D view

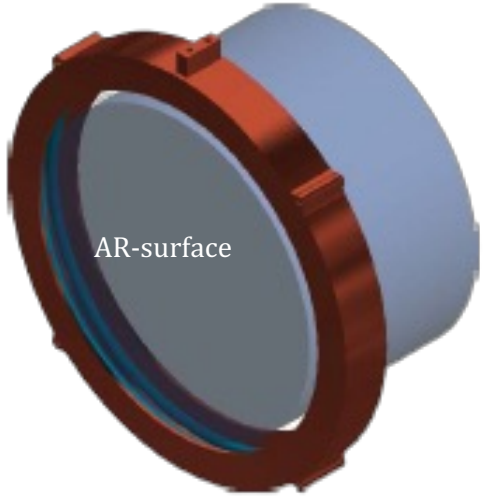

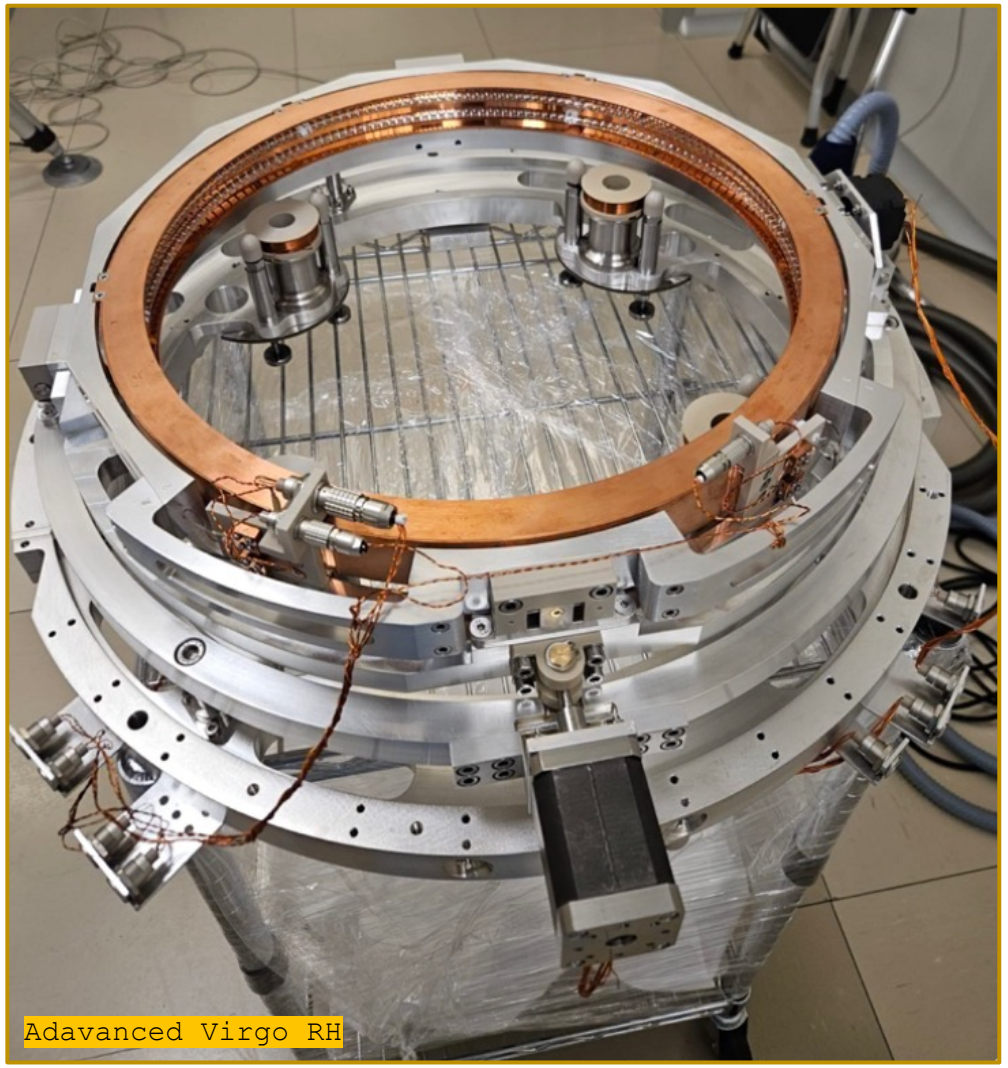

Ring Heater Simulations

- **RH-induced thermo-elastic deformation decreases the mirror RoC**

- **Simulation workflow:**

Temperature map [FEA] → HR surface deformation [FEA] → Gaussian-weighted quadratic fit → ΔRoC

1) Temperature distribution inside the ITM substrate for RH power P=7W

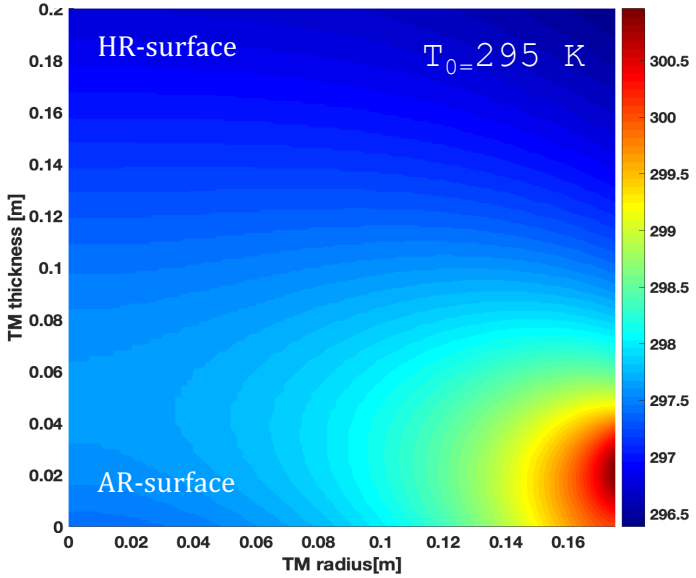

2) Thermoelastic mirror deformation

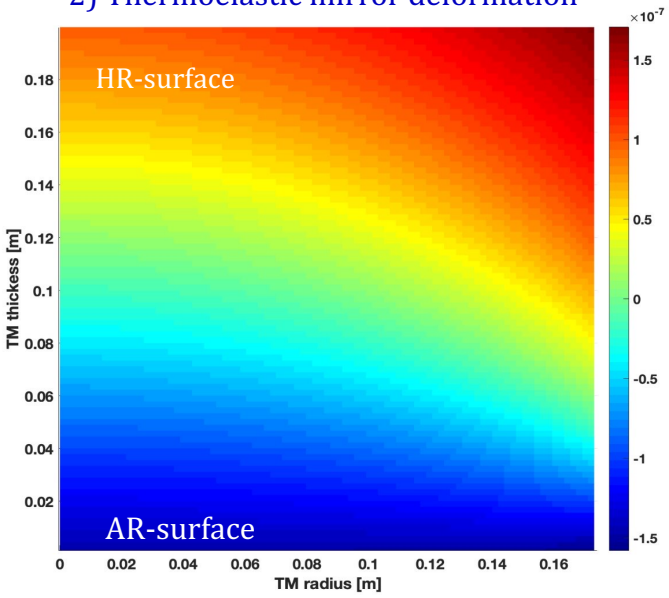

3) Gaussian-weighted quadratic fit

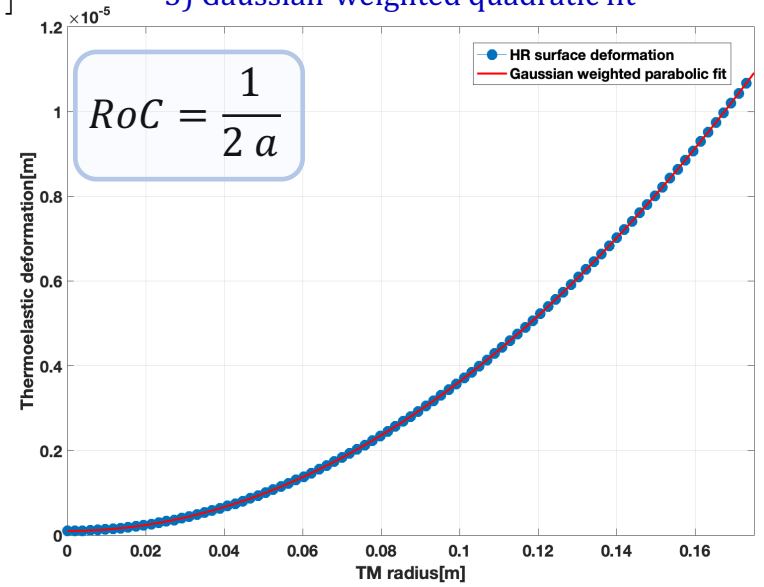

- Compensation is almost purely spherical (>98%)

- Typical RoC dynamics: ~ -2 m/W

CHRoCC RADIATIVE PROJECTOR

- **CHRoCC**: **C**entral **H**eating **R**adius of **C**urvature **C**orrection (Developed by EGO group)
- **Radiative actuator complementary to the RH increases mirror RoC (same effect as YAG heating)**
- Radiative element:
  black-body emitter + elliptical reflector

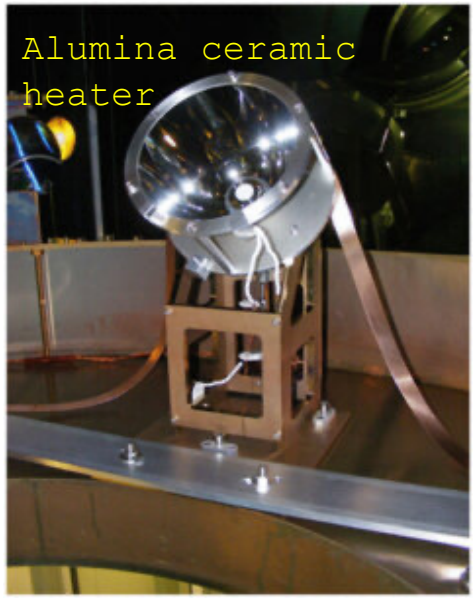

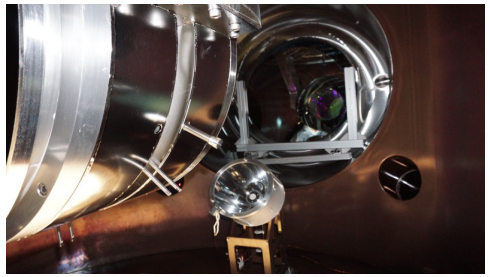

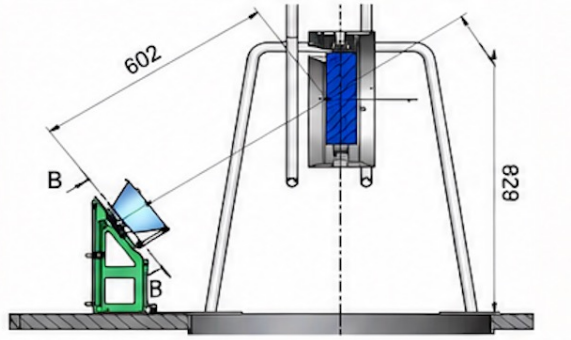

OPTICAL SIMULATION

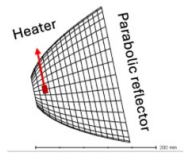

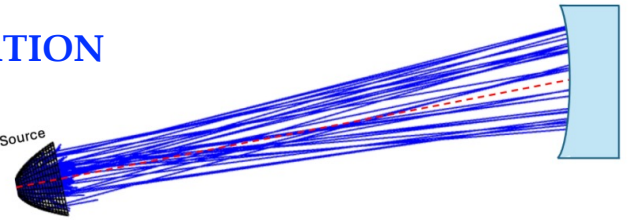

FEA SIMULATIONS

1) Temperature distribution inside the ITM substrate for CHRoCC power P=17W

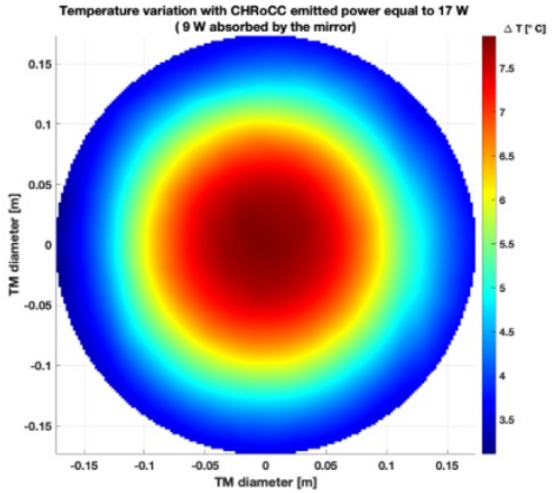

2) Thermoelastic mirror deformation

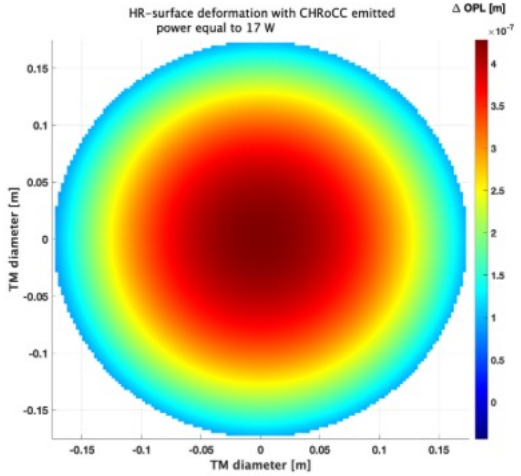

- Compensation is almost purely spherical

Hartmann-Wavefront Sensor (HWS)

- Measures wavefront variations relative to a reference wavefront
- Uses an uncoherent probe beam [fiber coupled super luminiscent diode (SLED)]
- In the image plane of the aberrated surface
- HWSs are used in two different configurations:
  - ON-AXIS
  - OFF-AXIS

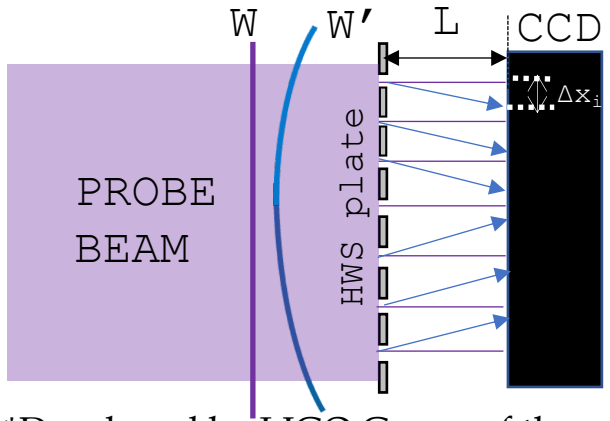

*Developed by LIGO Group of the University of Adelaide (Australia)

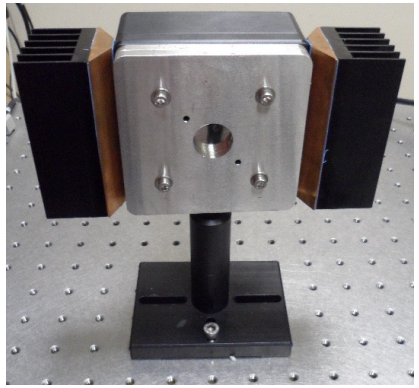

ON-AXIS SET UP

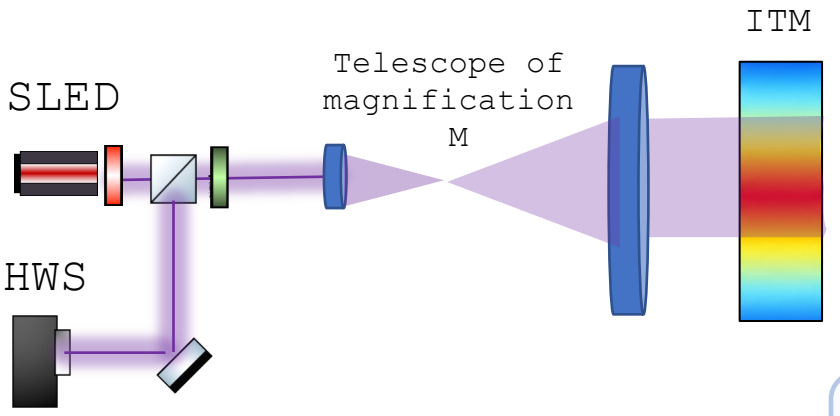

OFF-AXIS SET UP

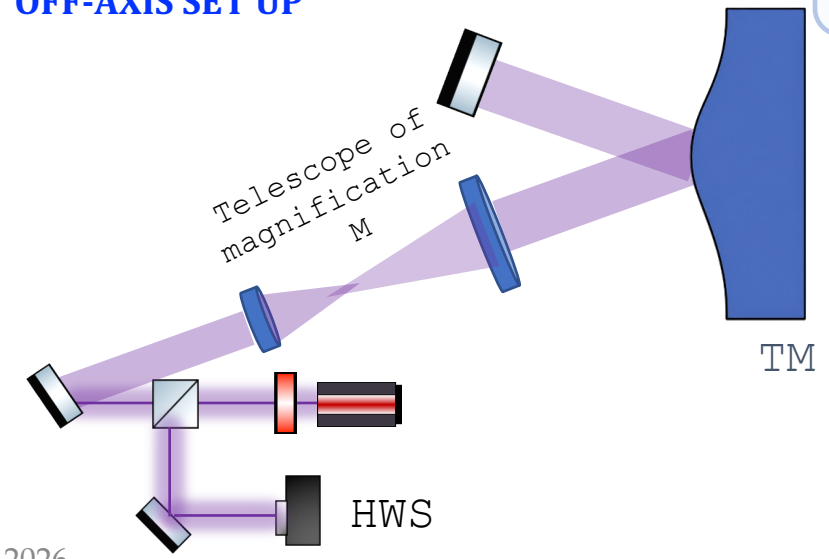

RoC relation:

$RoC_{TM} = M^2 RoC_{HWS}$

HWS-ON AXIS

- They are fundamental for the TCS pre-commissioning:
  - to align the CO_2 actuators on the CPs
  - to evaluate the absorption values in the test masses
  - to characterize all thermal actuators

- ITF locked at 25 W without TCS:
  → positive curvature;
- After engaging DAS:
  → curvature goes to zero;
- ITF unlocked with DAS ON:
  → negative curvature appears
- ITF relocked with DAS ON:
  → curvature equal to zero.

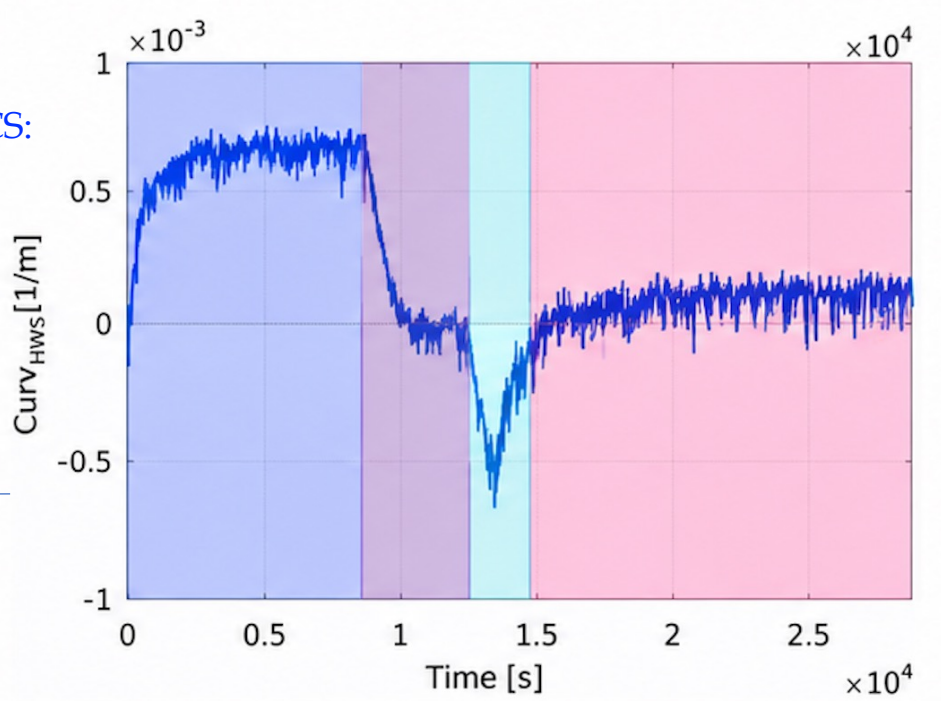

Central heating actuation overimposed on the RH one

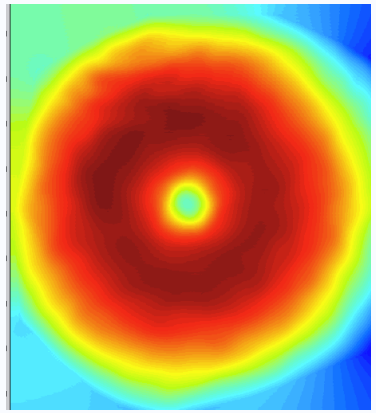

Example of absorption measurements in the input test mass of Advanced Virgo

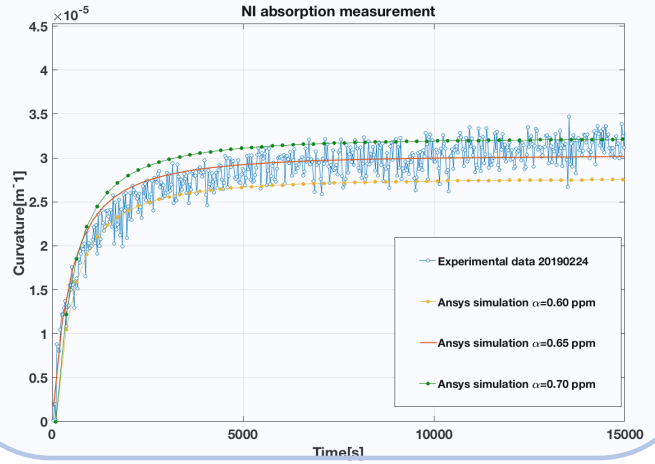

- Real-time monitoring of thermal curvature evolution

HWS-OFF AXIS

- Probe beam injected off-axis with respect to the ITF beam
- Sensitive to the HR-surface thermo-elastic deformation

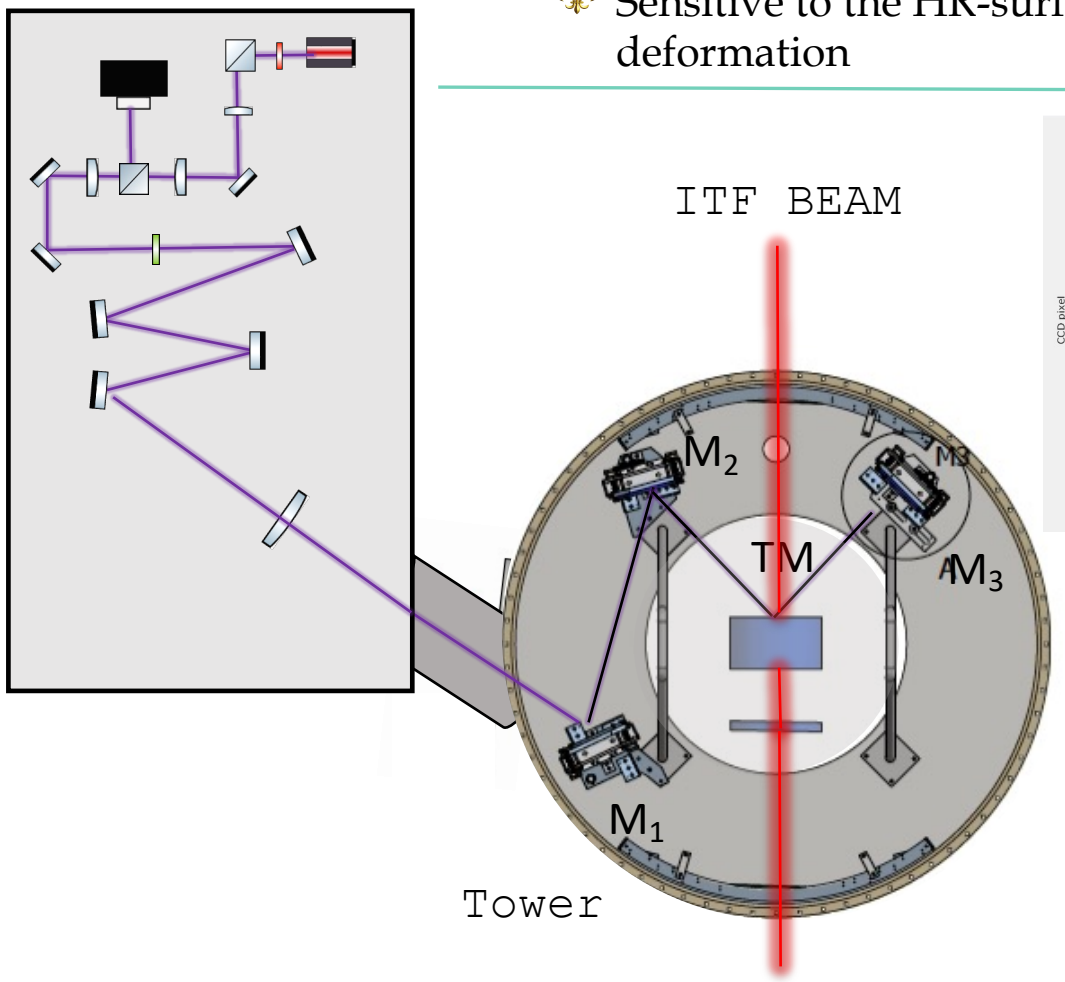

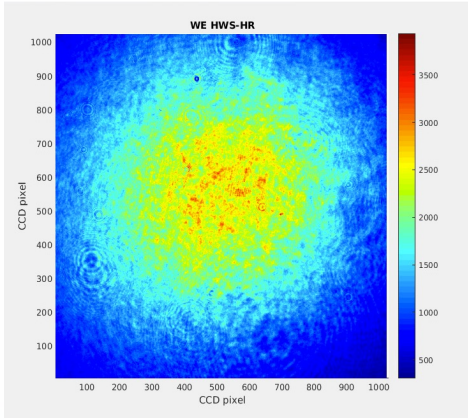

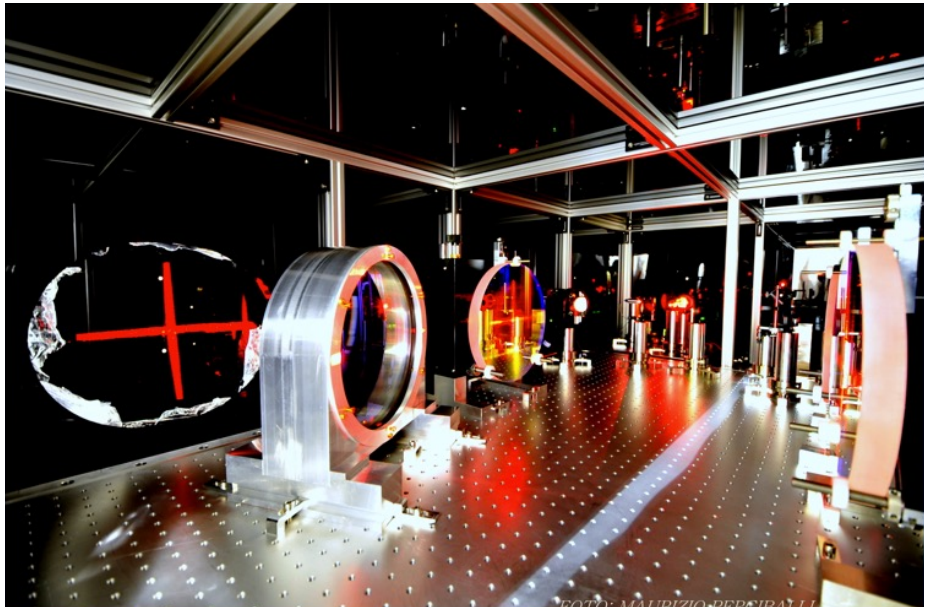

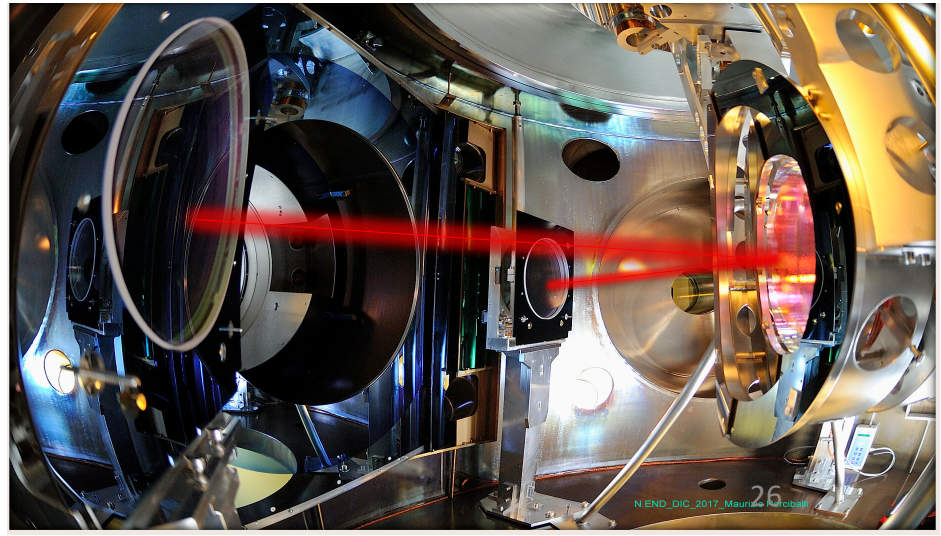

Credit by Maurizio Perciballi

Phase Cameras (PC)

- The phase camera (PC) senses aberrations in the beam propagating through the interferometer
- Two phase cameras are installed at the bright and dark ports of the interferometer
- Heterodyne detection allows independent measurement of the carrier, upper sideband, and lower sideband

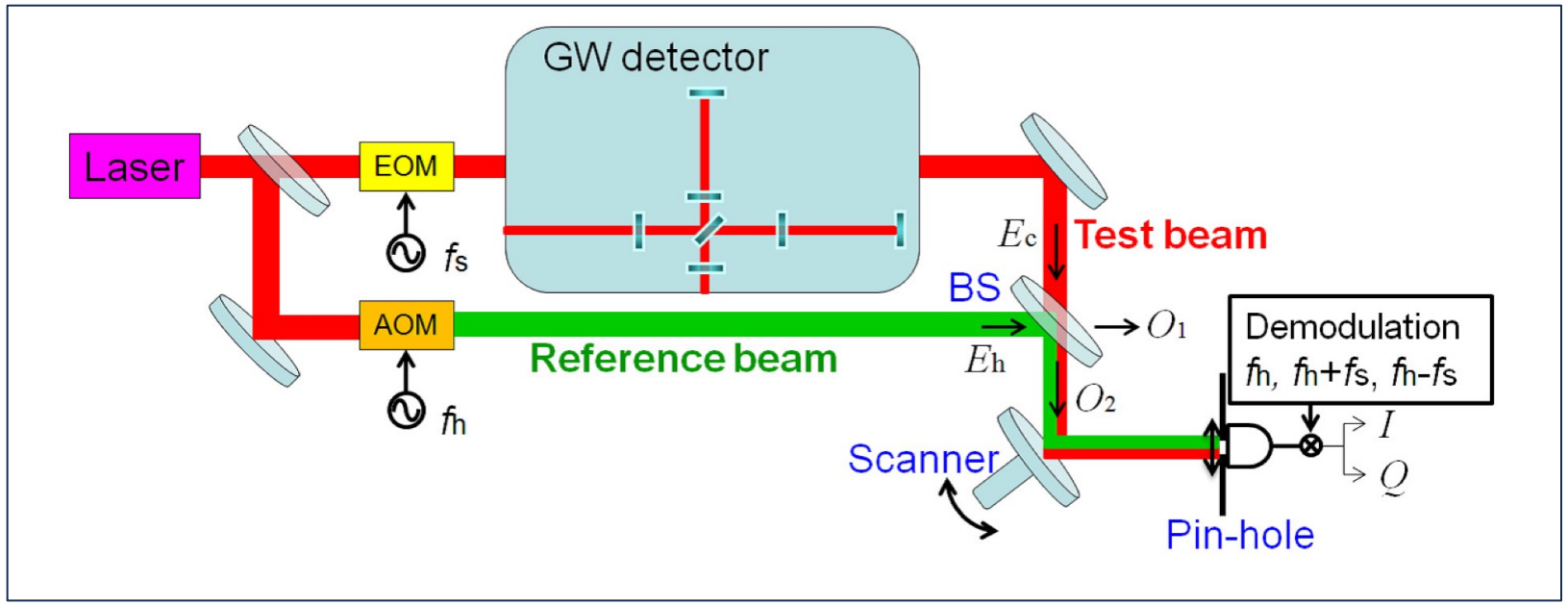

Example measurement

Carrier field on the
Dark Fringe with the ITF in
the final working point

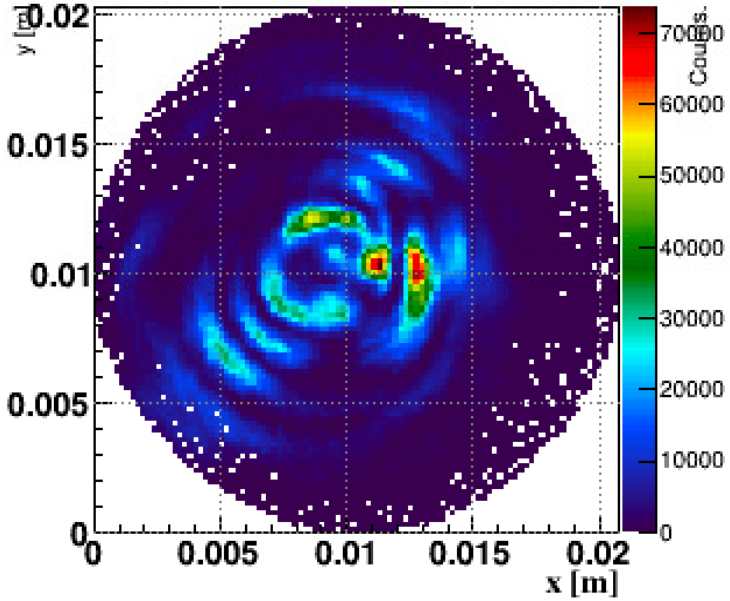

Advanced Virgo TCS

TCS ACTUATORS

CO_2 laser projectors
thermal lensing correction

Ring Heaters (RH)
thermoelastic deformation of the HR surface (RoC correction)

CHRoCC
fine tuning of the Radius of Curvature (RoC)

TCS SENSORS

HWS OFF-AXIS
Hartmann Wavefront Sensor on the HR surface: measures HR surface deformation

HWS ON-AXIS
Hartmann Wavefront Sensor in the recycling cavities: measures thermal lensing

Phase Cameras (PC)
monitor higher-order modes (carrier and sidebands) at the PRC and on the DP

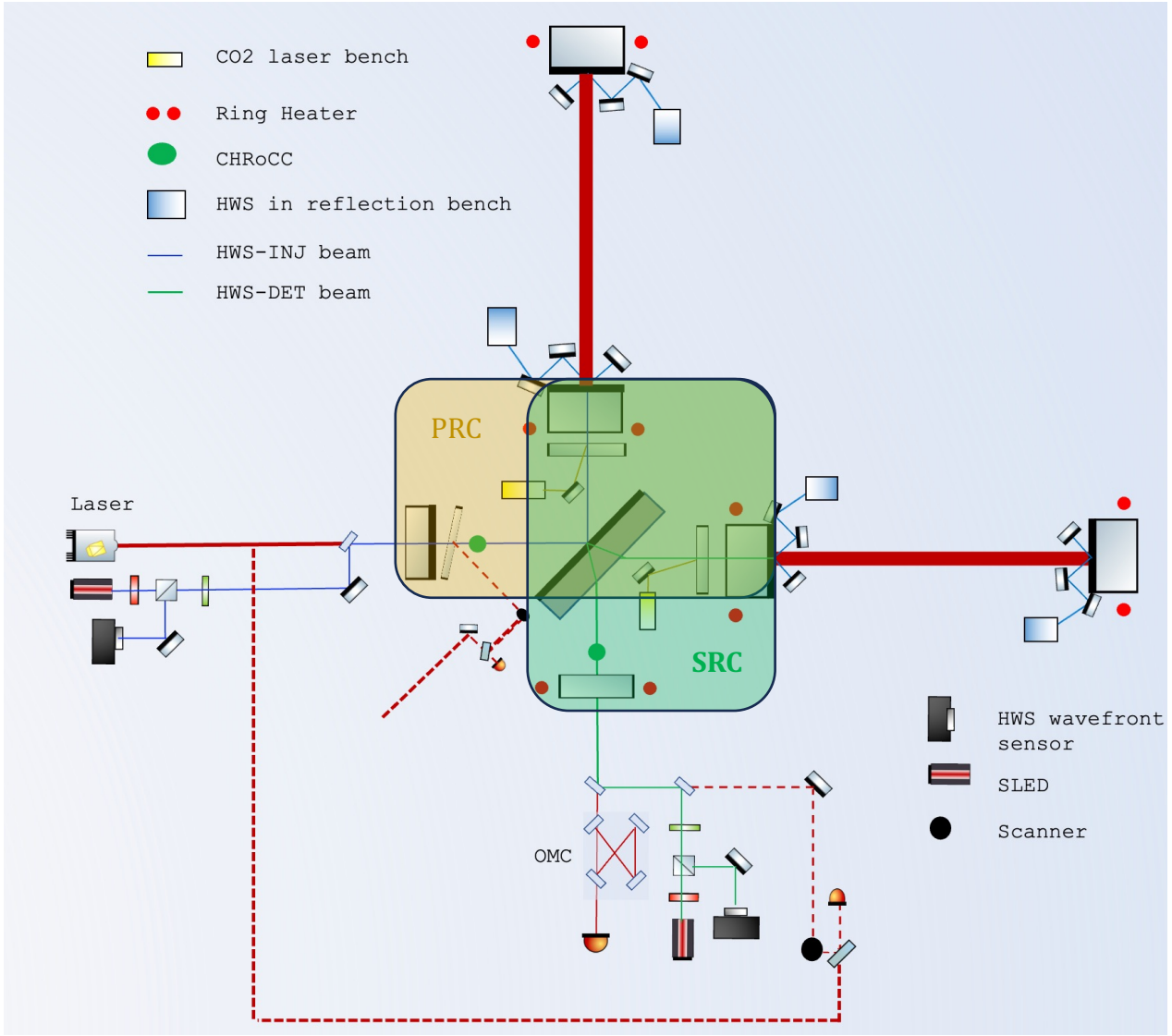

Point Absorbers (PA)

- Localized high-absorption regions on the HR mirror surfaces:
  - small
  - randomly distributed across the optics
  - characterized by optical absorption much higher than the average coating absorption
  - Possible origins:
    - coating defects (spectroscopic analyses revealed high concentrations of aluminium in several absorbers)
    - dust particles deposited during installation or handling
  - First identified in LIGO ITFs and later observed in Virgo as the circulating power increased

Examples of PA on LIGO mirrors observed under a microscope

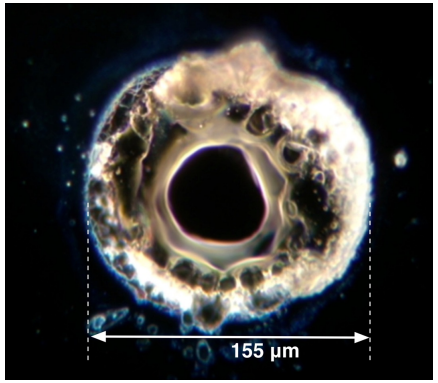

[Aidan F. Brooks, et al.. Appl. Opt. 60, 4047-4063 (2021)]

- Effects on the mirror:
  - Localized thermo-elastic deformation of the HR surface
  - Localized thermal lensing in the substrate

- Effects on the interferometer:
  - Generation of HOMs in both the FP and recycling cavities
  - Reduction of the circulating power in both the FP and recycling cavities
  - Degradation of the interferometer duty cycle and sensitivity

Point absorbers on AdV mirrors observed with a thermal camera and the HWS

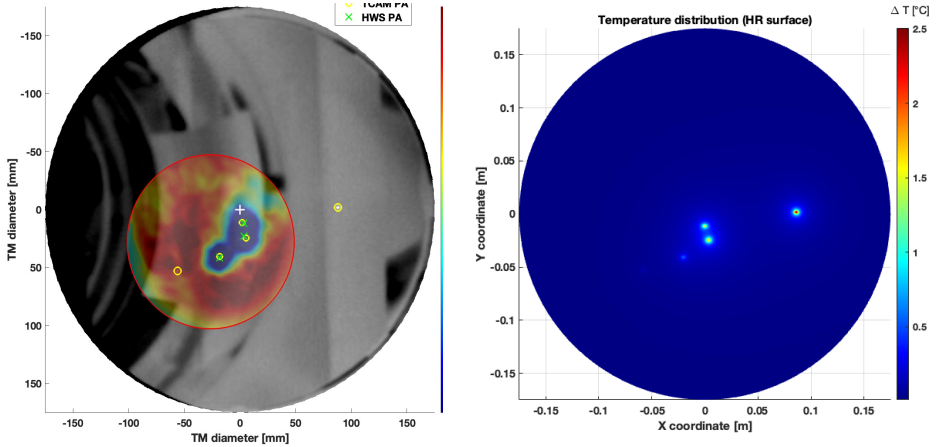

Point Absorbers compensation

- The correction strategy aims at reducing the thermal gradient induced by the point absorbers by heating the surrounding colder areas
- The correction principle is based on reproducing a target thermal deformation using a binary heating mask.
- Each square in the mask acts as an independent thermal actuator that can be either ON or OFF.
- The optimal mask pattern is reconstructed through the influence matrix formalism.

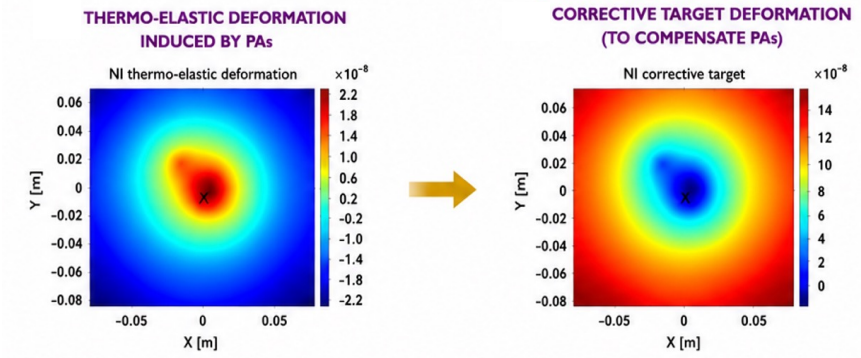

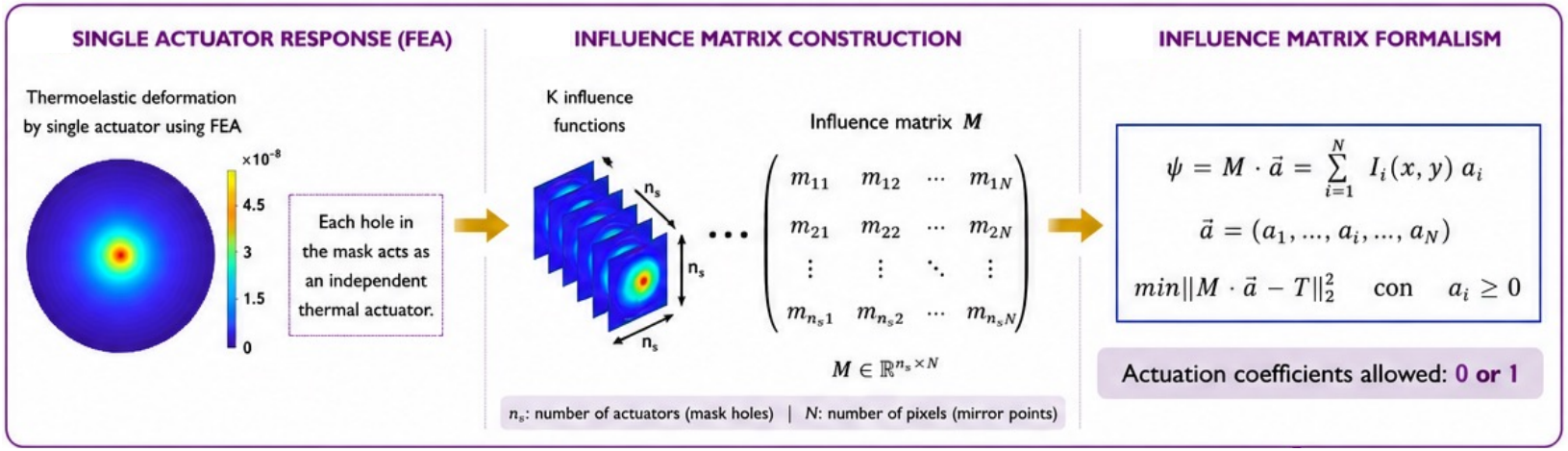

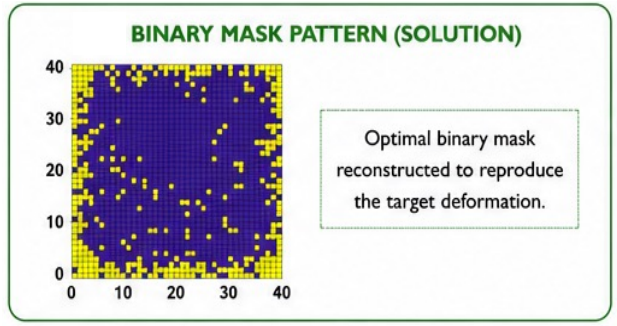

Point Absorbers actuator

- Radiative actuator conceptually similar to CHRoCC
- Radiative element:
  - black-body emitter
  - parabolic reflector
- The thermal pattern is first generated at the object plane and then imaged onto the test mass
- Installed in air outside the vacuum system
- The thermal radiation enters the tower through a ZnSe viewport

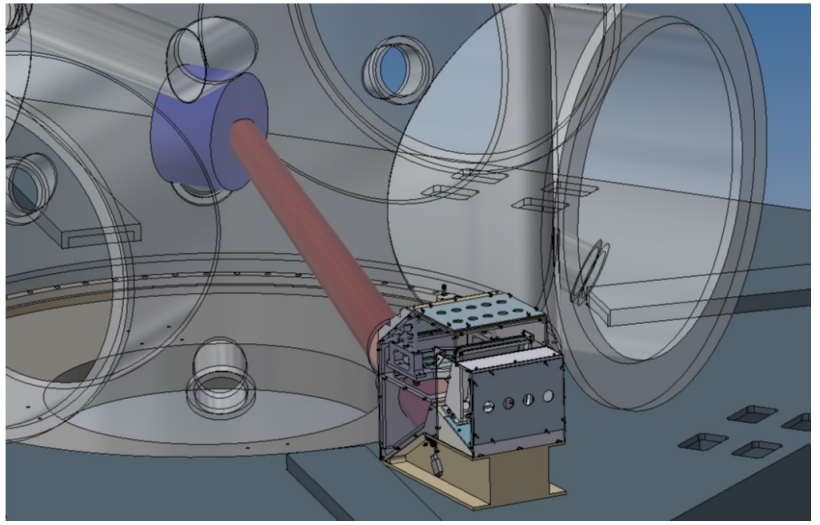

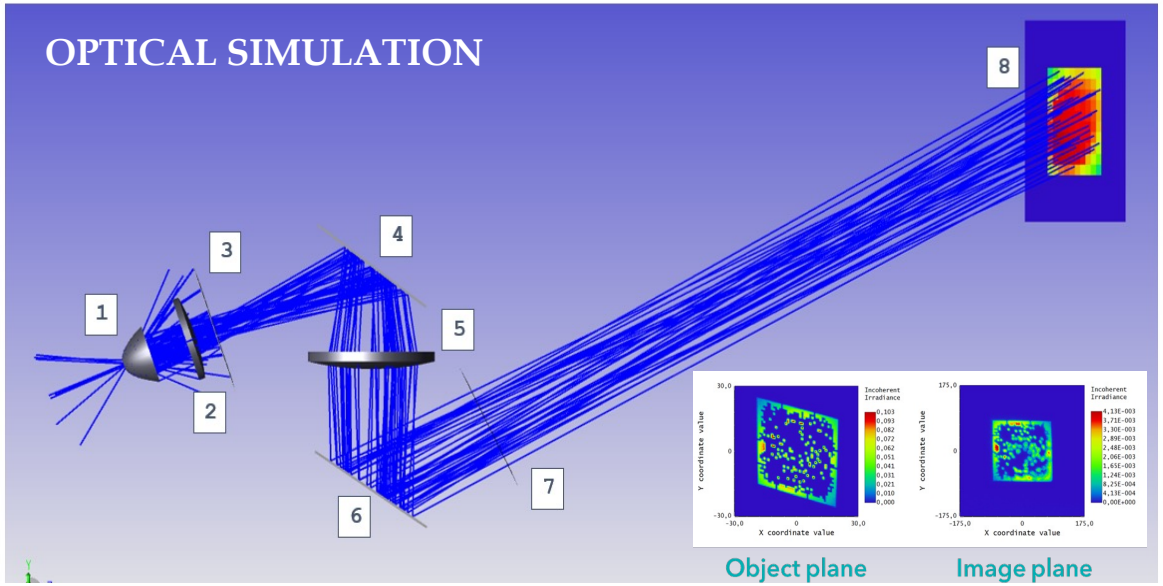

Experimental patterns

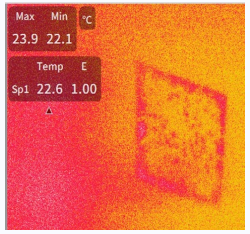

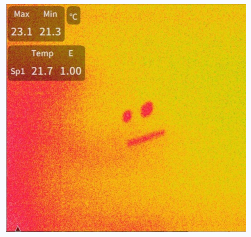

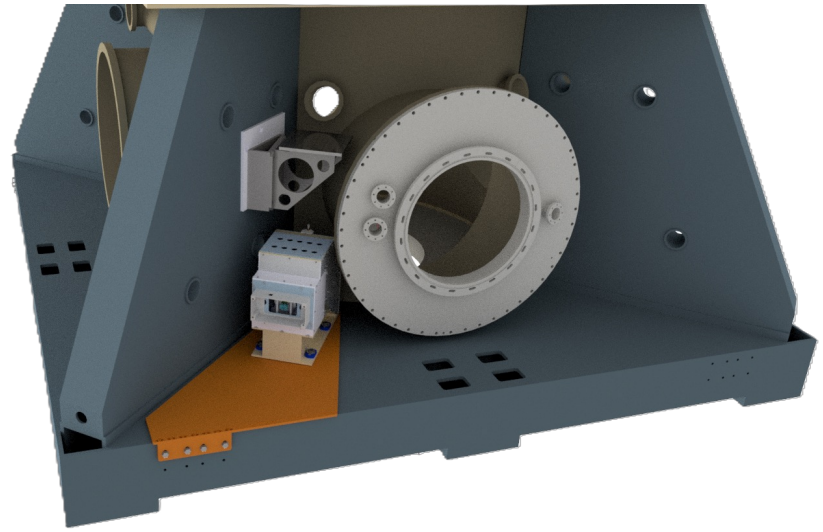

1: Parabolic reflector and ceramic heater
2: Focusing Germanium Lens
3: Binary mask
4-6: Steering mirrors
5: Imaging Germanium Lens (8")
7: ZnSe viewport
8: Test Mass

IPATSiA: Point Absorber simulator

- IPATSiA (Infrared Point Absorber Thermal Simulator Actuator)
- CO_2 laser system used to generate artificial localized thermal defects on the HR surface of the mirror
- Dynamic control of the artificial point absorber:
  - Position on the mirror surface
  - Size
  - Injected power
- Developed to study the interferometer response to localized defects
- IPATSiA further confirmed that HOMs generated by localized defects introduce additional noise in the Advanced Virgo sensitivity

CO2 beam projected on the mirror

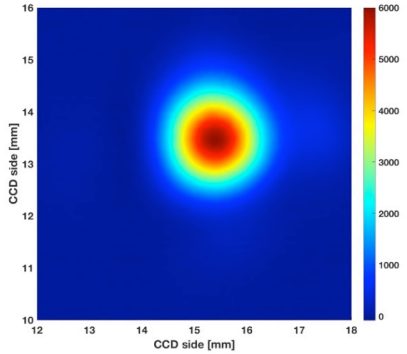

Optical layout

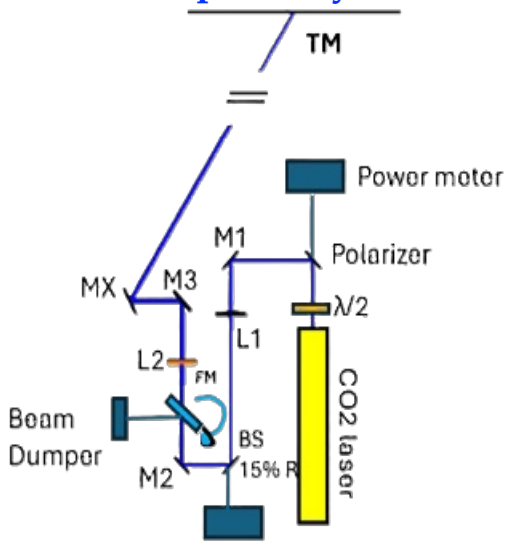

IPATSiA experimental setup

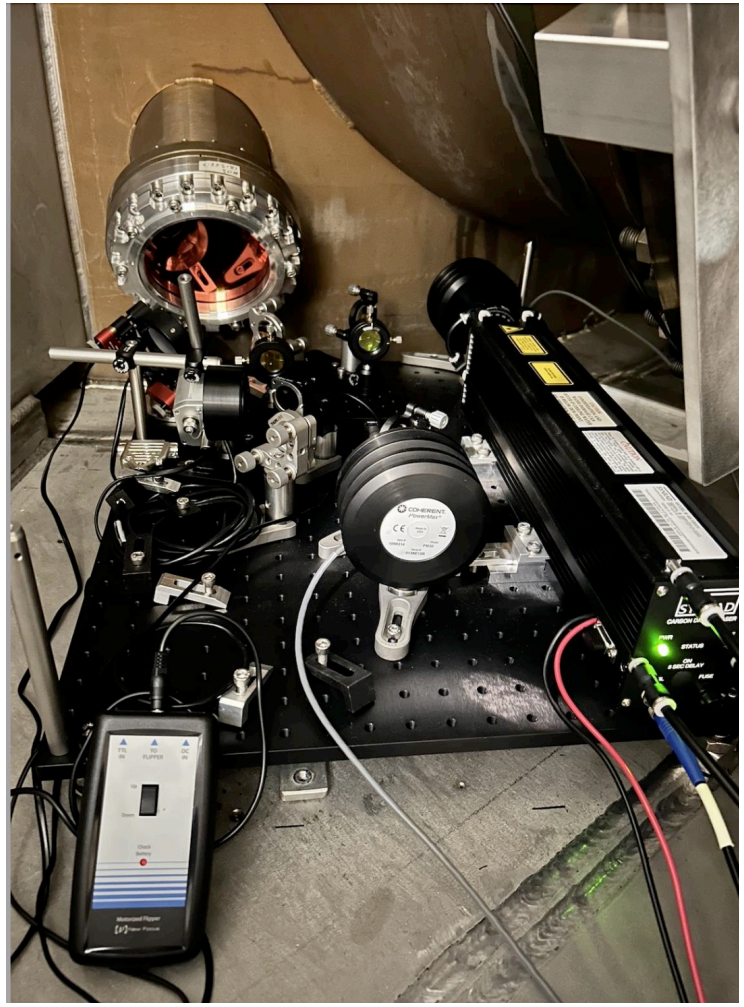

Next-generation wavefront actuators

- **A new generation of thermal actuators is being developed to address the MW-level circulating powers expected in future GW detectors such as Einstein Telescope.**

- **Thermal effects previously considered negligible will become increasingly critical**

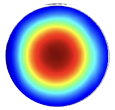

Current thermal actuators produce only axisymmetric compensation patterns. Only the spherical part of the thermo-elastic deformation on the HR-surface is componsated

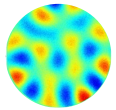

Localized defects generate non-axisymmetric and not-spherical aberrations (cold defects, DAS imperfections)

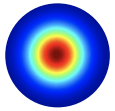

Aspherical residual thermo-elastic deformation increases with the circulating power

Example of complex residual deformation (non-axisymmetric)

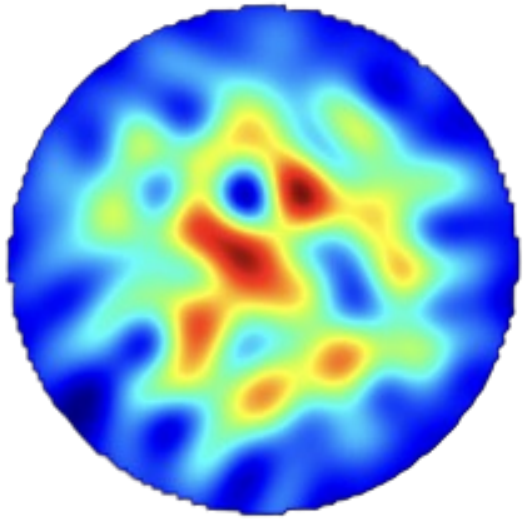

DEFORMABLE MIRROR (DM)

- **Goal**
  Use a deformable mirror coupled to the CO_2 laser to compensate localized defects by projecting complex non-axisymmetric heating patterns onto the CPs.

- **Method**
  DM shapes the phase of the CO_2 beam producing the required intensity pattern on the CP

- Long-standing expertise on deformable mirrors at Tor Vergata since 2016.

  - Latest deformable mirror tested: ***DM192-15*** (by ALPAO, 192 magnetic actuators with a grid layout)

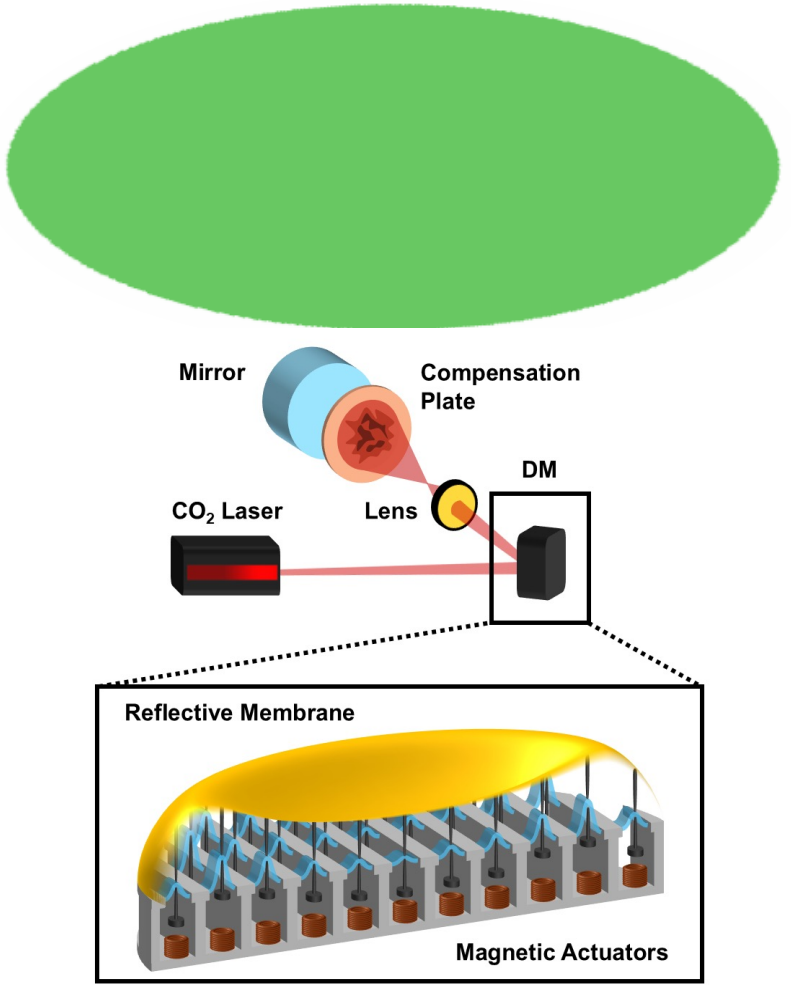

DEFORMABLE MIRROR (DM)

- The Modified Gerchberg–Saxton algorithm iteratively retrieves the phase map that must be applied by the deformable mirror in order to reproduce a desired intensity distribution.

Experimented tests ongoing in Tor Vergata Lab

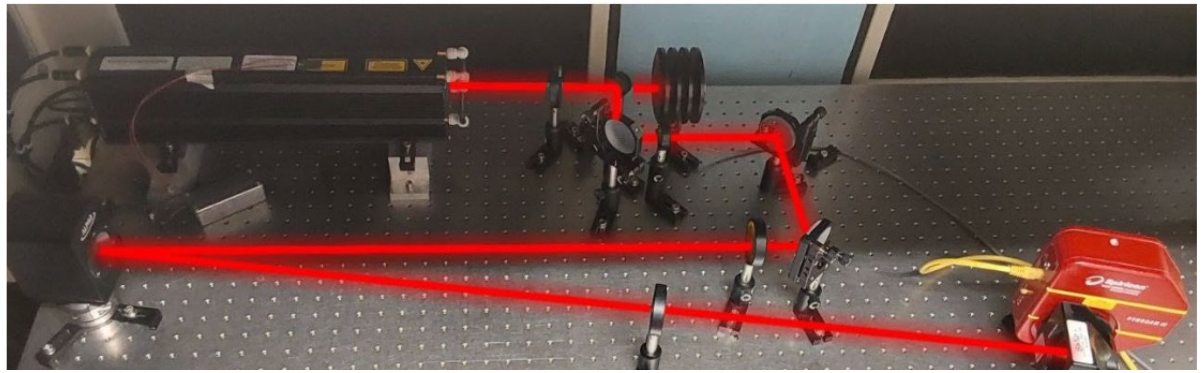

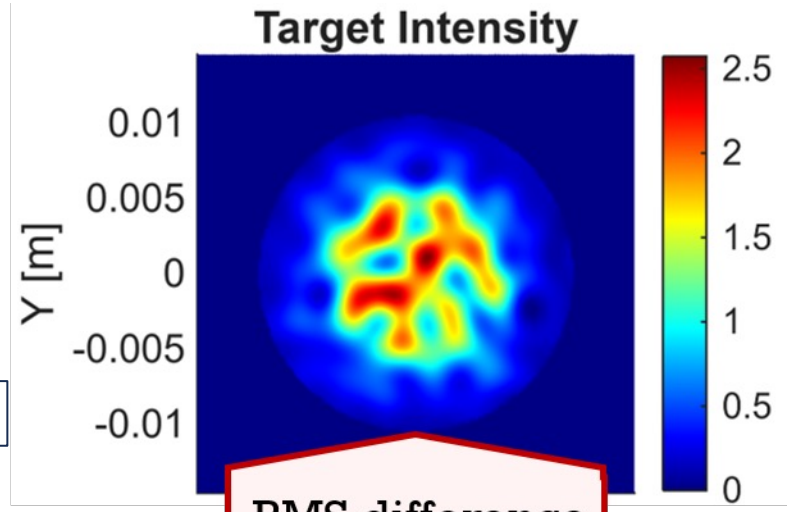

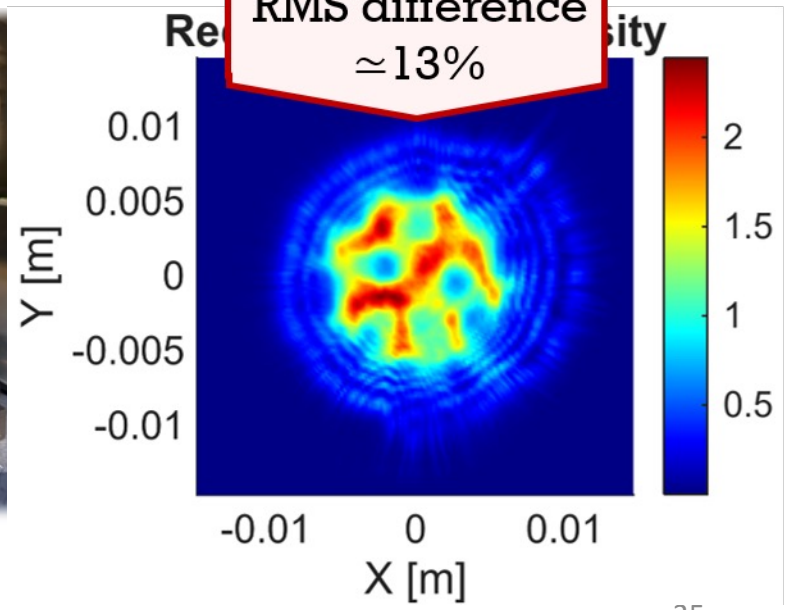

FRONT SURFACE TYPE IRRADIATOR (FROSTI)

- Residual aspherical thermo-elastic deformation increases with circulating power
- Residual aspheric deformation becomes limiting above P_cav~0.5–0.7 MW (VIR-0497D-22, LIGO-G2400546)
- LIGO developed a correction scheme based on an RH-like reflector
- An optimized profile projects the heating pattern directly onto the HR surface (FROSTI, DCC-G2402386)
- Gray-body radiation reshaped into an annular thermal pattern

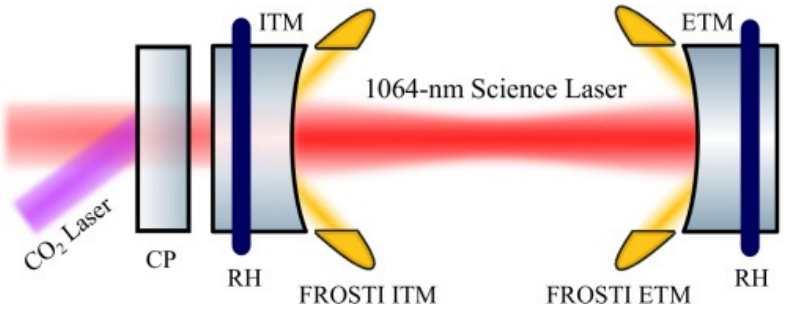

FROSTI prototype assembled and tested at LIGO

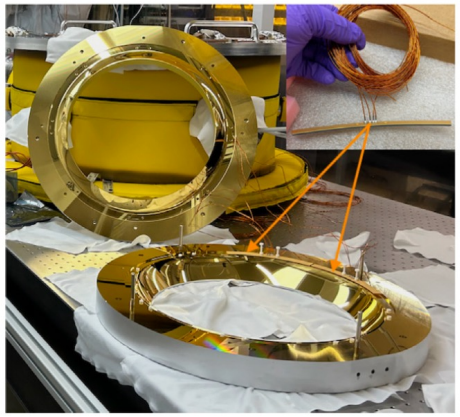

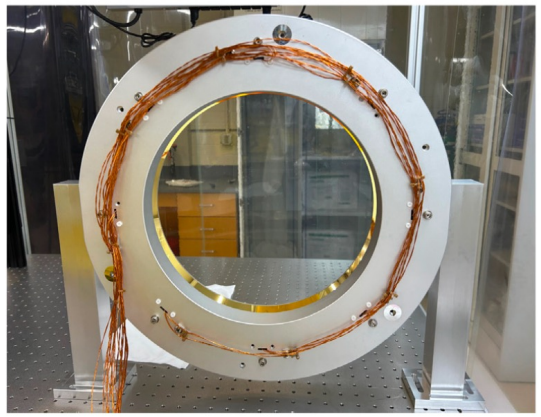

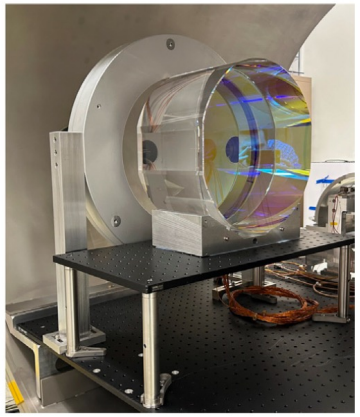

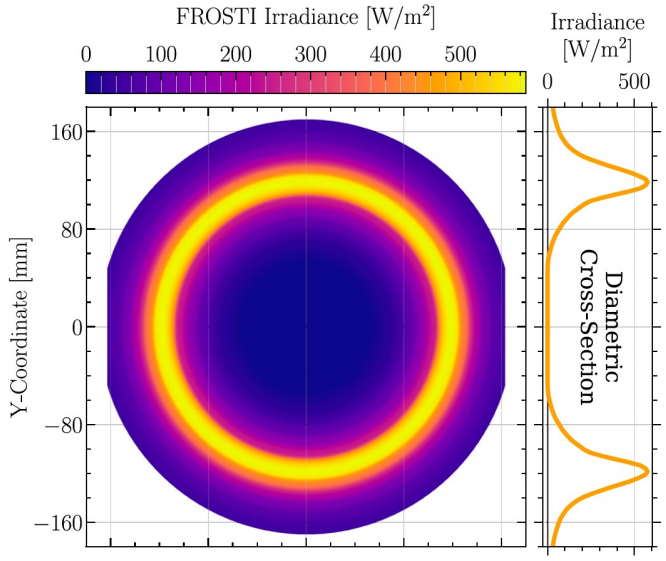

Take Away message

- Thermal effects are a major limitation for high-power GW interferometers.
- The Thermal Compensation System has proven to be fundamental for the operation of gravitational-wave interferometers, especially for Advanced Virgo, where the recycling cavities operate in a marginally stable configuration.
- Traditional TCS compensates mainly for first-order axisymmetric aberrations.
- At MW-level circulating powers, non-axisymmetric and higher-order aberrations are becoming increasingly critical.
- Thermal compensation is evolving toward adaptive correction of complex optical aberrations.

→ **New adaptive thermal actuators are under development for next-generation of GW detectors.**

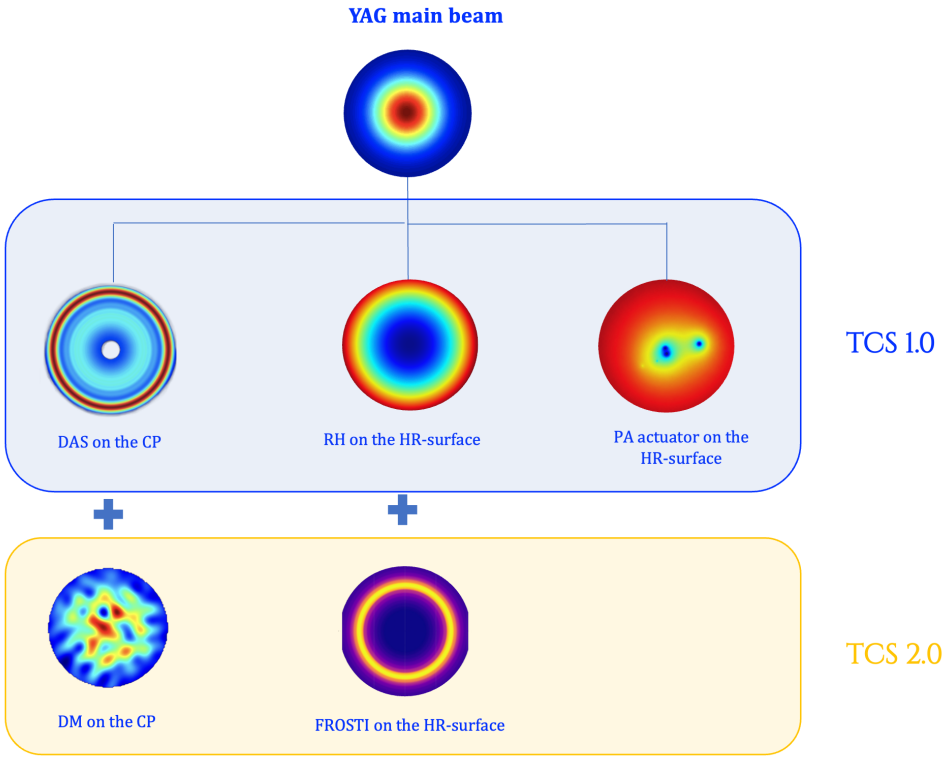


~ THANK YOU ~

ACRONYMS

RoC	Radius of Curvature
FP	Fabry-Pèrot
PRM	Power Recycling Mirror
PRC	Power Recycling Cavity
CP	Conpensation Plate
ITM	Input Test Mass
OPL	Optical Path length
DP	Dark Port
RH	Ring Heater
HWS	Hartmann Wavefront Sensor
PC	Phase Camera
DAS	Double Axicon System
CH	Central Heating
SLED	Superluminiscent Light Emitting Diode
DAS IN	DAS inner ring
DAS OUT	DAS outer ring
HOM	Higher Order Modes
CHRoCC	Central Heating Radius of Curvature Correction
DM	Deformable mirror
PA	Point Absorber

REFERENCES

[1] R. Lawrence et al., Adaptive thermal compensation of test masses in Advanced LIGO, Class. Quantum Grav. 19, 1803 (2003)
[2] The Virgo Collaboration, Advanced Virgo Baseline Design, Virgo internal note VIR-0027A-09, (2009).
[3] H. Luek et al., Thermal correction of the radii of curvature of the mirrors for GEO600, Class. Quantum Grav. 21, S985 (2004)
[4] Central heating radius of curvature correction (CHRoCC) for use in large scale gravitational wave interferometers, CQG, 30(5):055017, 2013
[5] Brooks A., Hartmann Wavefront Sensors for Advanced Gravitational Wave Interferometers, Ph.D. thesis, University of Adelaide, (2007)
[6] A. Rocchi et al., Thermal effects and their compensation in Advanced Virgo, J. Phys.: Conf. Ser. 363, 012016 (2012)
[7] I. Nardecchia, Control of optical aberrations in advanced gravitational wave detectors, PhD Thesis, 2016.
[8] L. van der Schaaf, K. Agatsuma, M. van Beuzekom, M. Gebeyehu, J. van der Brand, Advanced Virgo phase cameras, J. Phys.: Conf. Ser. 718 072008 (2016)
[9] David Voelz,Computational Fourier Optics, SPIE press